Continental Shelf Research ▮ (▮▮▮▮) ▮▮▮–▮▮▮

Contents lists available at SciVerse ScienceDirect

Continental Shelf Research

journal homepage: www.elsevier.com/locate/csr

Multiscale forecasting in the western North Atlantic: Sensitivity of model forecast skill to glider data assimilation

Avijit Gangopadhyay [a,*], Andre Schmidt [a], Laurie Agel [a], Oscar Schofield [b], Jenifer Clark [c]

[a] School of Marine Sciences, University of Massachusetts and School for Marine Science and Technology, University of Massachusetts, Dartmouth, 200 Mill Rd, Suite 325, Fairhaven, MA 02719, USA

[b] Coastal Ocean Observation Lab, Institute of Marine and Coastal Sciences, School of Environmental and Biological Sciences, Rutgers University, New Brunswick, NJ 08901, USA

[c] Jenifer Clark's Gulfstream, 3160 Lacrosse Court, Dunkirk, MD 20754, USA

ARTICLE INFO

Article history:
Received 29 April 2011
Received in revised form
15 September 2012
Accepted 26 September 2012

Keywords:
Glider data assimilation
Multiscale real-time forecasting
Observing simulation experiment (OSE)
Western North Atlantic
Mid-Atlantic Bight

ABSTRACT

A recently implemented real-time ocean prediction system for the western North Atlantic based on the physical circulation model component of the Harvard Ocean Prediction System (HOPS) was used during an observation simulation experiment (OSE) in November 2009. The modeling system was built to capture the mesoscale dynamics of the Gulf Stream (GS), its meanders and rings, and its interaction with the shelf circulation. To accomplish this, the multiscale velocity-based feature models for the GS region are melded with the water-mass-based feature model for the Gulf of Maine and shelf climatology across the shelf/slope front for synoptic initialization. The feature-based initialization scheme was utilized for 4 short-term forecasts of varying lengths during the first two weeks of November 2009 in an ensemble mode with other forecasts to guide glider control.

A reanalysis was then carried out by sequentially assimilating the data from three gliders (RU05, RU21 and RU23) for the two-week period. This two-week-long reanalysis framework was used to (i) study model sensitivity to SST and glider data assimilation; and (ii) analyze the impact of assimilation in space and time with patchy glider data. The temporal decay of salinity assimilation is found to be different than that of temperature. The spatial footprint of assimilated temperature appears to be more defined than that of salinity. A strategy for assimilating temperature and salinity in an SST-glider phased manner is then offered. The reanalysis results point to a number of new research directions for future sensitivity and quantitative studies in modeling and data assimilation.

Published by Elsevier Ltd.

1. Introduction

Ocean observing has advanced in the last decade from a ship-based expeditionary science to a distributed and observatory-based approach. This transition, which has been occurring over last decade (Glenn and Schofield, 2003, 2009), reflects the maturation of a wide range of observation platforms, data assimilative numerical models, and improved global communications (Schofield et al., 2012). The expanding suite of observational assets include remote sensing (satellite: Halpern, 2000, aircraft: Lomax et al., 2005, HF Radar: Crombie, 1955; Barrick, 1972; Barrick et al., 1977), fixed location assets (moorings: Hayes et al., 1991, Weller et al., 2000, seafloor cables: Schofield et al., 2002, Kunze et al., 2006), and Lagrangian platforms (AUVs: Blackwell et al., 2008, gliders: Sherman et al., 2001, Eriksen et al., 2001, Webb et al., 2001, drifters: Niiler et al., 2003, floats: Davis et al., 1992, Gould et al., 2004). As the number of deployed platforms increases there is a growing need to aggregate the data and coordinate the sampling among the individual systems in order to create a system-of-systems. This will require the development of coherent software networks that allow a distributed group of sensors and/or scientists to operate as a group.

The integration of software systems is currently under development. For example, the U.S. National Science Foundation's Ocean Observatory Initiative (OOI, http://www.oceanleadership.org/programs-and-partnerships/ocean-observing/ooi/) has focused a significant effort on developing a sophisticated cyberinfrastructure (CI) that binds the physical observatory, computation, storage and network infrastructure into a coherent system-of-systems. This CI is also being designed to provide a web-based social network, enabled by real-time visualization and access to numerical models, to provide the foundation for adaptive sampling science. The OOI cyber-development has chosen to utilize a spiral design strategy, allowing the oceanographic community to provide input during the construction phase with the strategy of utilizing existing ocean observing networks. For this effort, the OOI utilized an existing

* Corresponding author. Tel.: +1 508 910 6330; fax: +1 508 910 6374.
E-mail address: avijit@umassd.edu (A. Gangopadhyay).

0278-4343/$ - see front matter Published by Elsevier Ltd.
http://dx.doi.org/10.1016/j.csr.2012.09.013

ocean observing network in the Mid-Atlantic Bight (MAB) as part of the National Oceanographic and Atmospheric Administration's (NOAA) Integrated Ocean Observing System (IOOS) in November 2009. The goal was to use this network to conduct an observation simulation experiment (OSE). The objective was to use the oceanographic testbed to support field operations of ships and mobile platforms aggregate data from fixed platforms, shore-based radars, and satellites; and offer these data streams to data-assimilative forecast models. Additional goals were to use multi-model forecasts to guide glider missions and coordinate satellite observing, and to demonstrate the ability to conduct two-way interactions between the sensor web and predictive models. While previous studies have focused on the phytoplankton dynamics during spring and/or spring transition (Ryan et al., 1999a, 1999b, 2001), this field effort was conducted to collect data on the status of the Mid-Atlantic shelf in early winter, when the winter phytoplankton bloom occurs (Schofield et al., 2010).

This paper uses data collected during the OSE to investigate the forecast sensitivity to glider data assimilation. One goal of this study is to understand and develop a protocol for future similar test experiments based on a careful reanalysis during the OSE period. An interesting new result from the assimilation analysis is the apparent difference of spatial and temporal scales of impact between temperature and salinity. These behavioral differences might lead to future areas of research in modeling and assimilation.

This paper is organized as follows. The methodology is presented in Section 2 and the analysis of the real-time forecasts made during the OSE period is presented in Section 3. A reanalysis based on systematic glider data assimilation is presented in Section 4, followed by a summary and discussion in Section 5.

2. Approach and methods

A distributed community of ocean scientists provided the CI team with regional surface datasets, a surface current mapping network, a constellation of fixed and taskable satellites, a fleet of autonomous Slocum gliders, a multi-vehicle network of autonomous underwater vehicles, and five different data-assimilative forecast ocean models that tested the OOI software. An overview of the OSE effort is described by Schofield et al. (2010). The OSE was a multi-institutional, multi-investigator effort. Various OSE groups coordinated satellites, multiple gliders, and an AUV during the OSE period of October 26 through November 17, 2009. A data and model portal was assembled (http://ourocean.jpl.nasa.gov/CI) (Wang et al., in this issue) for multi-model ensemble forecasting and glider guidance decision-making efforts.

2.1. Regional data streams

A large suite of satellites were used during this study. The satellites provided multiple passes of sea surface temperature and ocean color observations. The data was downloaded and processed at both the NASA Jet Propulsion Lab and the Rutgers Coastal Ocean Observation Lab. Data was processed in near real-time (hours) and posted to the data portal.

The surface currents on the MAB are measured by an extensive network of high frequency CODAR networks array. The CODAR network consists of twelve 5 MHz systems located along the northeast of the United States. The HF Radar uses the Doppler Shift of a radio signal backscattered off the ocean surface to measure the component of the flow in the direction of the antenna. The network provides surface current estimates to a depth of 2.4 m (Stewart and Joy, 1974).

2.2. Gliders

Slocum gliders are an autonomous underwater scientific platform (Webb et al., 2001) manufactured by the Teledyne-Webb Research Corporation. They are 1.8-m long, torpedo-shaped, buoyancy-driven vehicles with wings that enable them to maneuver through the ocean at a forward speed of 20–30 cm s^{-1} in a sawtooth-shaped gliding trajectory. Each Slocum glider has a payload bay that houses a SeaBird conductivity–temperature–depth sensor and includes space for a range of additional sensors. The glider acquires its global positioning system (GPS) location every time it surfaces, which is programmable and was set to call-in every 3 h for the purposes of this study. By dead reckoning along a compass bearing while flying underwater, estimates of depth averaged current can be calculated based on the difference between the glider's expected surfacing location and the actual new GPS position. Depth averaged current measurements obtained in this manner have been validated against stationary Acoustic Doppler Current Profiler data (Glenn and Schofield, 2003).

During this experiment, four Webb gliders were deployed by Rutgers University and the University of Delaware. The gliders were deployed prior to the start of the experiment on Nov 1 2009 and operated for two weeks. During that period the gliders traversed 1673 km underwater collecting 23,332 vertical profiles. The data collected were analyzed for various process studies including phytoplankton productivity (Schofield et al., 2012) and sediment re-suspension during fall storms (Miles et al., in this issue).

2.3. Numerical model

One of the five numerical models employed during the OSE is the SMAST-HOPS (School for Marine Science and Technology—Harvard Ocean Prediction System) real-time forecast system, which has been operational since March 9, 2009, providing a 7-day ocean forecast for the large-scale Gulf Stream region from Cape Hatteras to 55°W, including the Gulf of Maine and the Mid-Atlantic shelf region. The other four models were: (i) the New York Harbor Ocean Prediction System (NYHOPS) for MARACOOS (Bhushan et al., 2009; Georgas and Blumberg, 2009); (ii) the regional ocean modeling system for MARACOOS (Wilkin et al., 2005); (iii) the regional ocean modeling system from USGS (Warner et al., 2008); and (iv) the MIT multidisciplinary simulation, estimation and assimilation system (MSEAS) (Lam et al., 2009; Haley and Lermusiaux, 2010). The SMAST-HOPS operational system (described by Schmidt and Gangopadhyay, 2012, in this issue, SG12 henceforth; Brown et al., 2007a, b; Robinson et al., 2001) regularly assimilates satellite SST and, when available, MARACOOS glider-measured 4-D water properties to produce weekly 3-D nowcast and forecast MARACOOS regional temperature maps (see http://www.smast.umassd.edu/modeling/RTF/index.php). Four forecasts were provided during the OSE period, assimilating all available data from SST and the four gliders.

The horizontal structure of the SMAST-HOPS operational model domain consists of 131×83 grid points with 15 km resolution, extending from 30.5°N to 47.93°N in the meridional and from 80.54°W to 54.23°W in the zonal direction. The vertical structure of the model is resolved by 16 levels that are distributed according to a topography-following "double sigma" transformation described by Lozano et al. (1996) and Sloan (1996). The open boundary conditions for tracers and velocity are based on Orlanski (1976); and the horizontal subgridscale processes are parameterized using a set of scale-selective Shapiro filters: 4-1-1 (fourth order, one time, every time step) for velocity and tracers, a 2-2-1 for vorticity and 2-1-1 for streamfunction. The time step

Please cite this article as: Gangopadhyay, A., et al., Multiscale forecasting in the western North Atlantic: Sensitivity of model forecast skill to glider data assimilation. Continental Shelf Research (2012), http://dx.doi.org/10.1016/j.csr.2012.09.013

Table 1
Objective analysis parameters for glider data initialization and assimilation with a 12-h time window.

	Initialization		Assimilation	
	Synoptic	Mean	Synoptic	Mean
Decay (km)	60	180	30	90
Zero crossing (km)	120	360	60	180
Time decay (day)	90	1000	10	80

used in all runs was 225 s. Some of the important numerical model parameters and their values are given in Table 1 of SG12. Note that this model system has yet to incorporate a real-time river runoff input.

The operational forecasting system is built on the feature-oriented initialization scheme developed by Gangopadhyay et al. (1997) for the Gulf stream meander and ring (GSMR) region and for the Gulf of Maine and Georges Bank (GOMGB) region (Gangopadhyay et al., 2003). The feature-oriented methodology is explained in detail for the GSMR–GOMGB region by SG12, and has now been developed for many other regions of the world ocean including the South Atlantic (Calado et al., 2008), the Trinidad North Brazil current (Schmidt et al., 2011) and the California current system (Gangopadhyay et al., 2011). Briefly, FORMS methodology (Gangopadhyay and Robinson, 2002) requires (i) the development of analytical–empirical formulation of the synoptic-dynamic characters of features such as fronts, eddies, gyres and currents etc. called 'feature models,' and then (ii) implementation of a multiscale melding using objective analysis of calibrated synoptic feature models (with available satellite and in-situ data) with background mean state to create the ''most knowledgeable'' nowcast. For the MARACOOS implementation, the deep-water feature model set for GSMR (Gulf Stream, Deep western boundary current, warm and cold core rings, southern and northern recirculation gyres; see Gangopadhyay et al. (1997) for details) is melded with the shallow-water feature model set in the GOMGB region (Maine coastal current, Georges Bank tidal front, Wilkinson–Jordan–Georges basin gyres, northeast channel inflow and great south channel outflow; see Gangopadhyay et al. (2003) for details), and further supplemented with the Levitus climatology as the background in a multiscale objective analysis framework. The initialization field is dynamically adjusted with wind forcing and used in an SST-assimilative forecast model using the methodology described by Brown et al. (2007b). The model is forced with atmospheric fields (surface momentum flux, surface heat flux, surface water flux and shortwave radiation) from the global forecast system (GFS) at 0.5-degree resolution for 7 days. Several products are used for assimilated SST, including 3-day composite products from the Johns Hopkins University/Applied Physics Laboratory, AVHRR passes processed by the MARACOOS group at the University of Delaware College of Marine and Earth Studies, and daily and multi-day blended products from remote sensing systems. See SG12 for full details of this implementation and the model skill validation using drifters and GS axis locations from satellite observation.

While the OSE period was a test of the development and implementation of the cyberinfrastructure, the data collected during this period provided a valuable opportunity to reanalyze and understand various aspects of underlying processes and methodologies, which depend on data, models and model-data synthesis exercises. One of them is the focus of this paper, in which we assess the impact of glider data assimilation on the SMAST-HOPS model simulation. Such an exercise would make possible the design of better and more effective schemes for real-time assimilation utilizing satellite, glider and other in-situ observations in future OSEs.

Assimilation of data in numerical ocean models has been in practice for over couple of decades now (Carter and Robinson, 1987; Robinson et al., 1989; Derber and Rosati, 1992; Ezer and Mellor, 1992; Fukumori and Malanotte-Rizzoli, 1995). A comprehensive set of studies on the different approaches to data assimilation in ocean modeling for the early nineties were compiled by Malanotte-Rizzoli (1996). More recent advances in data assimilation include, among many, the works with the regional ocean modeling system (3DVAR and 4DVAR) (Li et al., 2008a, 2008b; Chao et al., 2009; Broquet et al., 2009; Veneziani et al., 2009), with the navy's coastal ocean model (Barron et al., 2007; Shulman et al., 2007, 2009), and with the Harvard Ocean Prediction System (Lozano et al., 1996; Lermusiaux, 1999, 2002; SG12) and the MIT multidisciplinary simulation, estimation and assimilation aystem (MSEAS) (Lam et al., 2009; Haley and Lermusiaux, 2010). With increasing computing power, more mathematically elegant and computationally demanding methods such as extended Kalman Filters, ensemble Kalman Filters (EnKF) are being adapted to ocean and atmosphere modeling at a rapid pace (Kalnay, 2003; Ott et al., 2004; Hunt et al., 2004; Kalnay et al., 2007; Evensen, 2009). However, while the techniques are improving, the availability of data for assimilation in the ocean models still remains sparse and infrequent. This necessitates generating suitable initialization and assimilation fields from a set of irregularly occurring observations in both space and time. Specifically, a set of decay scales in space and time (based on data auto-correlations) is generally applied to construct the initialization and assimilation fields (Mooers, 1999). It is also expected, that the impact of such patchiness would result in an assimilated field where errors will dominate away from the center of assimilation. In this study, we attempt to understand this impact facilitated by the availability of the patchy glider data set in a selective region in the reanalysis mode.

3. Assimilation of glider data in model forecasts

The sensitivity of the model simulations to glider data assimilation is examined over the two-week period (Nov 2 through Nov 16). This section describes the Gulf Stream system during the OSE period, the glider data and the initialization and assimilation protocols. Section 4 then describes the numerical experiments and the results.

3.1. The gulf stream system during OOI–CI–OSE

The FORMS-based initialization for the SMAST-HOPS operational system requires an ocean analysis. This analysis for the western North Atlantic provides the surface characterizations of the locations, shapes and sizes of various features such the Gulf Stream, its rings, and the shelf-slope front. The specific product used for the SMAST-HOPS model is Jenifer Clark's Gulfstream (http://users.erols.com/gulfstrm/), which is a typical ocean analysis created primarily from the NOAA polar orbiting thermal infrared satellite imagery. The data are false-colored based on different sea surface temperatures. Other sources of data include altimetry, drifting and fixed buoys, model output, and sea surface isotherm analyses. The analyses extend from 80°W to 45°W and from 50°N to 30°N. The images are then subjectively analyzed by an oceanographic expert. They are generated once a week and have been analyzed since 1980. The analyses have improved over the years due to inputs and feedback from various stakeholders such as sailboat racers, coast guard search and rescue, fishermen,

Please cite this article as: Gangopadhyay, A., et al., Multiscale forecasting in the western North Atlantic: Sensitivity of model forecast skill to glider data assimilation. Continental Shelf Research (2012), http://dx.doi.org/10.1016/j.csr.2012.09.013

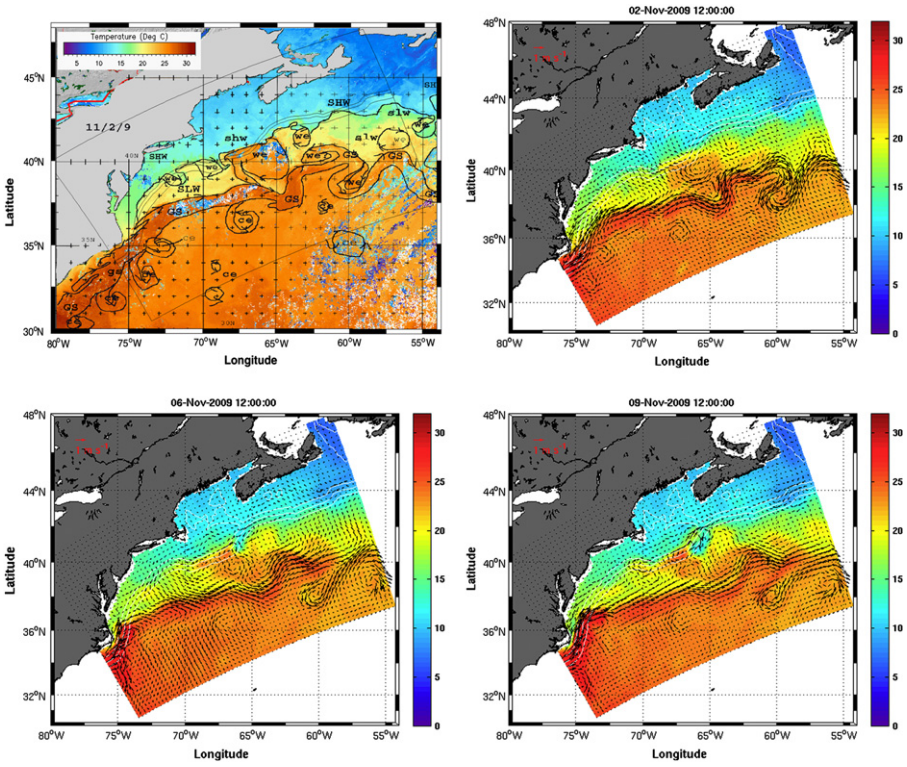

Fig. 1. Weekly Jenifer Clark analysis of Gulf Stream ring and eddy positions, with cold core rings and eddies noted as "ce" and warm core rings and eddies noted as "we" (top-left) for Nov 02, 2009.The SMAST-HOPS forecasts for Nov 2nd, Nov 6th and Nov 9th are shown in the other three panels.

scientists, forecast modelers, yacht deliveries, ocean rowers, swimmers, etc.

The week-long forecasts are issued generally by wednesday morning; monday 0-h is a typical model initialization state, with SST assimilation carried out on monday afternoon or on Tuesday morning. The forecast fields (temperature, salinity, currents) are available at www.smast.umassd.edu/modeling/RTF/MARCOOS for different levels at 6-hourly intervals for the full domain, and for zoom domains of the Mid-Atlantic shelf and the Gulf of Maine. To provide high-resolution, nested forecasts for the mission control of the AUV and glider fleets, the forecast data in netCDF format (CF-compliant) were made available from the OPeNDAP-enabled THREDDS server http://aqua.smast.umassd.edu:8080/thredds/catalog/models/catalog.html.

The configuration of the Gulf Stream system on November 02, 2009, as the study period begins, is shown in Fig. 1. The left panel shows the Jenifer Clark analysis, with outlines of the Gulf Stream and its filaments spreading out to the recirculation gyres and each independent ring. During the OOI–CI–OSE, the Gulf Stream system north of 32°N and west of 55°W includes 6–7 warm and 6–7 cold eddies, and a large meander from 65°W to 55°W. The meander shifts and changes shape over the 2-week period as it absorbs a large warm core ring and casts off a cold-core ring. The SMAST-HOPS forecasts for Nov 2, 6 and 9 are shown in Fig. 1 b–d. During these forecasts the SST and Glider data were assimilated in a strategic reanalysis to understand the behavior of assimilated fields after glider data assimilation.

3.2. Description of the glider sampling

The tracks of the gliders, showing the coverage area, are delineated in Fig. 2. The individual tracks for RU05, RU21, RU23 and UD134 are distinguished by color. The three Rutgers gliders

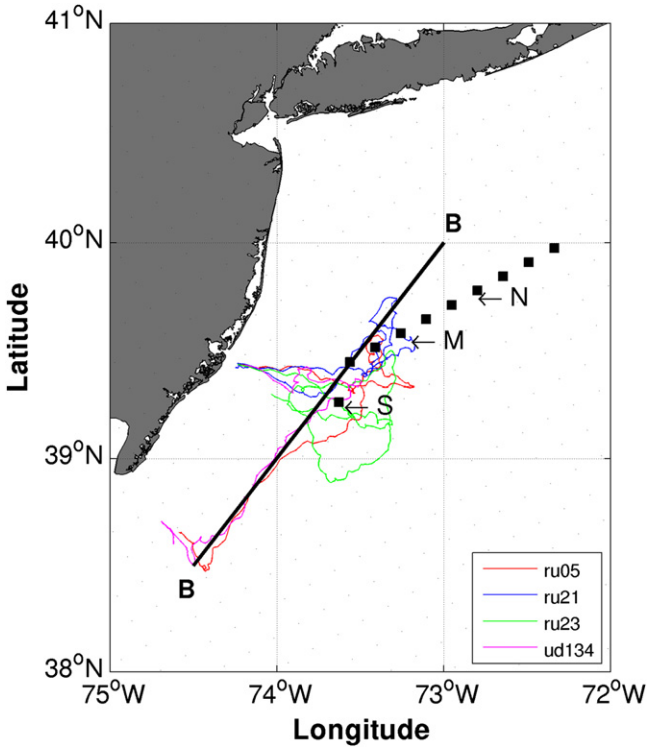

Fig. 2. Tracks of the three gliders (RU05, RU21 and RU23) used for initialization and assimilation of the 02 Nov 2009 SMAST-HOPS run. The tracks span from 30 Oct 2009 to 17 Nov 2009. Glider UD134, not used in the HOPS model, is also shown. The points marked by south (S), middle (M) and north (N), are where the spatio-temporal impact analysis of glider data assimilation is carried out. (For interpretation of the references to color in this figure legend, the reader is referred to the web version of this article.)

Please cite this article as: Gangopadhyay, A., et al., Multiscale forecasting in the western North Atlantic: Sensitivity of model forecast skill to glider data assimilation. Continental Shelf Research (2012), http://dx.doi.org/10.1016/j.csr.2012.09.013

(RU05, RU21 and RU23) were deployed off the New Jersey coast on October 26, and moved across the shelf to near the 50-m isobath within the first 3–4 days. All of them were then used for CI–OSE control experiments (Schofield et al., 2010) and were guided in different directions before recovery. For example, after following the cross-shelf path, RU05 (red) was guided northward during Nov 6–9, then southward in the second week, and finally was recovered near Delaware Bay on Nov 17. RU23 (green) zigzagged during the OSE across the 50-m isobath and was recovered on Nov 17 near its original deployment site. RU21 (blue) started from the same location, moved in a northeastward direction and was engaged in sampling fine-scale features (Schofield et al., 2012, in this issue). UD134 (pink) was deployed later on Nov 6, followed a track similar to that of RU05 (red) for the latter part of the 2-week period, and was also recovered on Nov 17 2009. The sensitivity to assimilation was studied along the line of the black rectangles and is described later.

3.3. Initialization and assimilation methodologies with glider data

For the purpose of initialization, the temperature and salinity data from RU05, RU21 and RU23 between Oct 26 and Nov 2 were melded with the standard operational FORMS-derived initialization field (SG12). The melding was done by carrying out a multiscale objective analysis (OA) in which the synoptic glider data were statistically merged with the FORMS initialization following well-established procedure (Brown et al., 2007a; BG07 henceforth; SG12). The OA parameters, such as the correlation scale and decay scales of choice for the glider data, are summarized in Table 1. The total sampling coverage for Oct 26–Nov 1 is shown in Fig. 3a. This process of melding available glider observations over a week (or less) at initialization of the dynamical model run is also known as 'assimilation at initialization.'

The sequential assimilation protocol for SST is explained in detail by SG12 (see their Section 3.3 and equation 1 therein). Briefly, the OI assimilation is a data-fusion methodology, where the observation (SST or Glider T/S) is assimilated in the model using a time-varying weighting function within each assimilation cycle. Subsequent glider data were assimilated at regular intervals of 12 h. Examples of glider data locations used for assimilation for a selected set of days are shown in Fig. 3b–f for Nov 4, 6, 8, 10, and 12, respectively. Initial fields of salinity and associated error fields are presented in Fig. 4. The contrast between glider salinity and climatology-derived background is much more pronounced than that between the corresponding temperature fields (not shown). This is because the assimilation of glider temperature is smoothed by the SST-assimilation from satellite observations. The subsurface projection of the satellite-derived SST field also helps reduce such contrast between glider and background temperature.

The weighting assimilation scheme for SST is described by BG07 and SG12 in detail. The weights for assimilating the glider data are presented in Fig. 5. Specifically, to allow for the internal dynamical adjustment of the assimilative variable, our approach is to distribute the field over a temporal window with variable weights. The 12-h Glider data is thus slowly amplified from its 20% value (weight of 0.2) on the 6th hour (prior to the observation hour) to its 90% value (weight of 0.9) on the 12th hour and then decays for next 6 h. This ramp-up and decay-down strategy is cycled every 12 h allowing for continuous and sequential assimilation of glider data within the observation window.

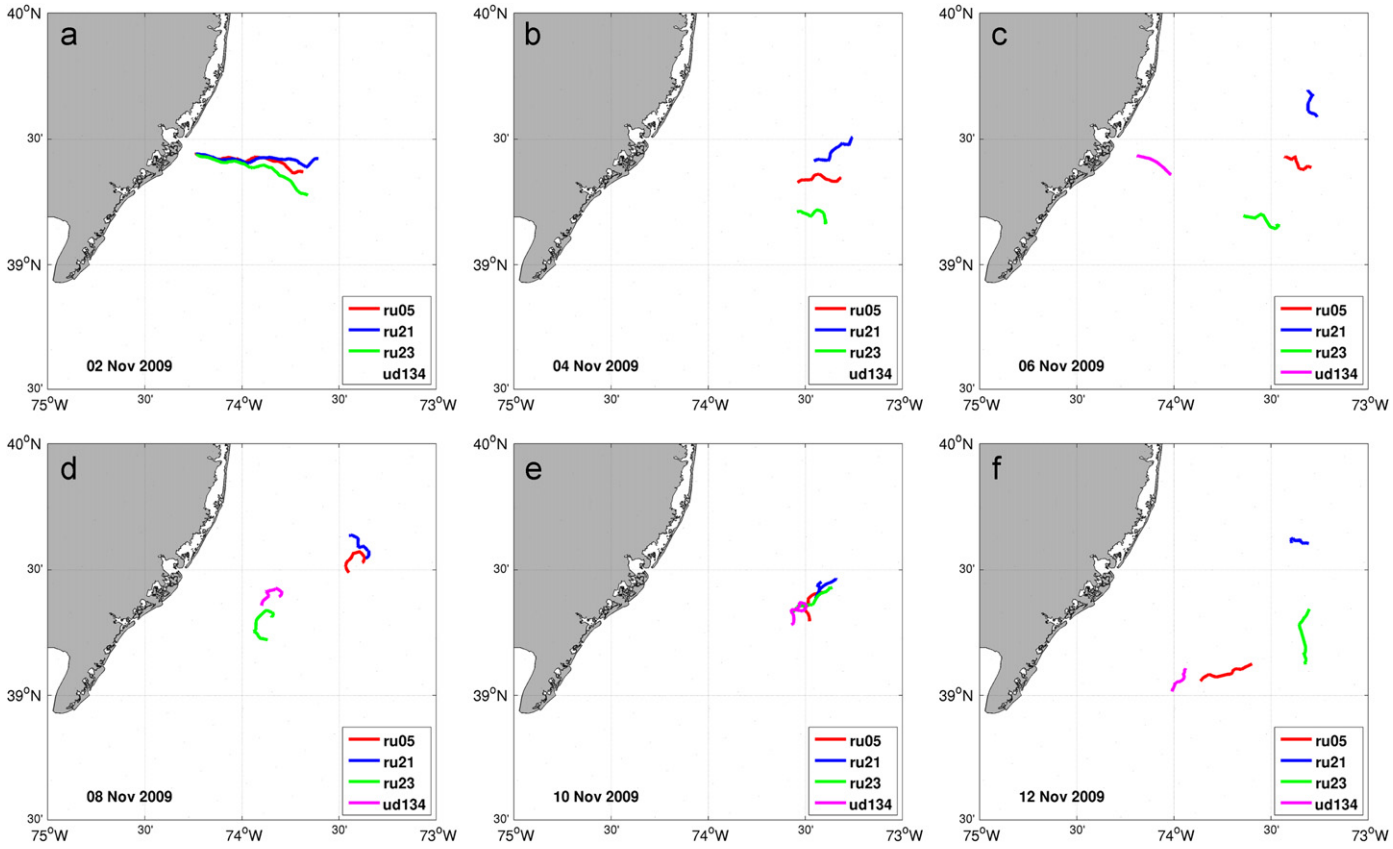

Fig. 3. Position of glider data used in the (a) initialization of the SMAST-HOPS 02 Nov 2009 run, and the assimilation of glider data for (b) 04 Nov 2009, (c) 06 Nov 2009, (d) 08 Nov 2009), (e) 10 Nov 2009, and (f) 12 Nov 2009. The initial field incorporates data collected from 30 Oct 2009 to 02 Nov 2009. The assimilation fields incorporate 12 h of glider data, centered on 0000 UTC.

Please cite this article as: Gangopadhyay, A., et al., Multiscale forecasting in the western North Atlantic: Sensitivity of model forecast skill to glider data assimilation. Continental Shelf Research (2012), http://dx.doi.org/10.1016/j.csr.2012.09.013

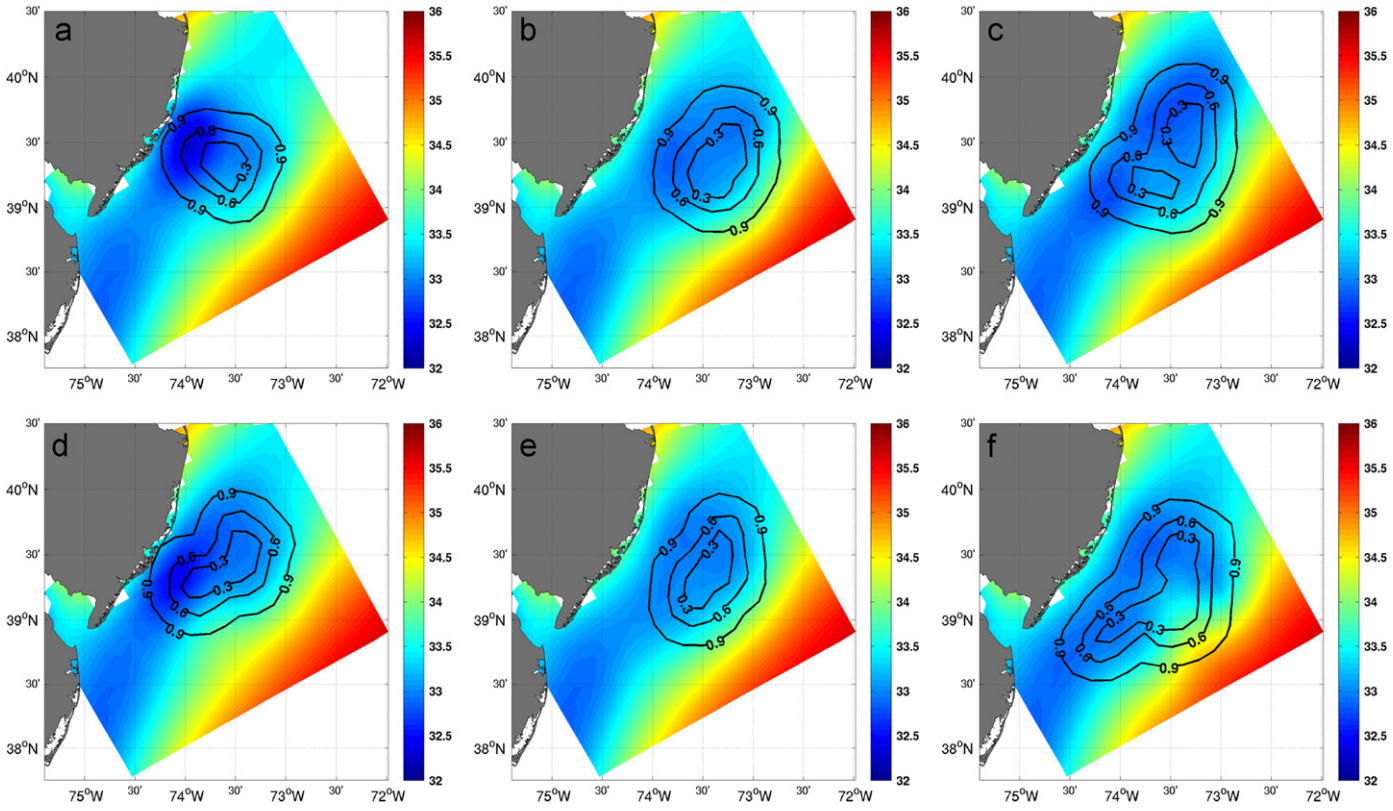

Fig. 4. OA salinity fields assimilated into SMAST-HOPS 02 Nov 2009 run for (a) 02 Nov 2009 (b) 04 Nov 2009 (c) 06 Nov 2009 (d) 08 Nov 2009 (e) 10 Nov 2009, and (f) 12 Nov 2009. Error is shown as contours.

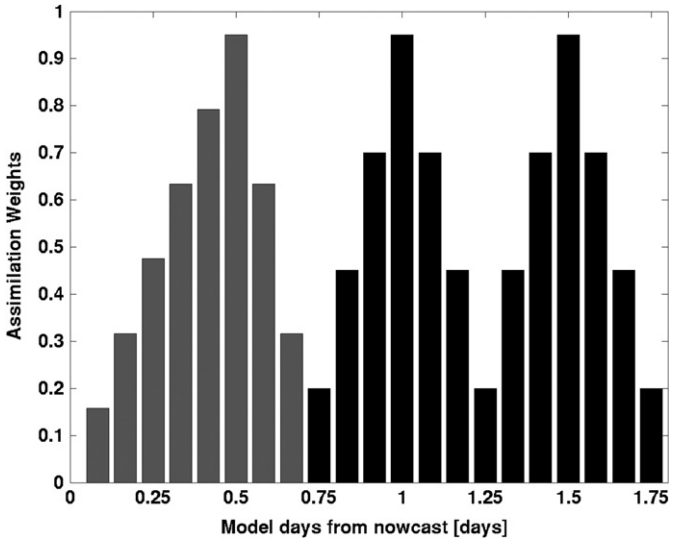

Fig. 5. Assimilation scheme used for SMAST-HOPS 02 Nov 2009 run, showing the weights used for SST (grey), and glider data (black) on the model days. Note that the glider assimilation is repeated with the same cycle as shown here after day 1.75.

It is instructive to analyze the differences between the glider profiles and the objectively analyzed profiles. Overall, the mean rms differences between the OA and glider data for temperature and salinity are comparable for all the gliders at all depths (Fig. 6). The depth-averaged rms difference between OA and the glider for temperature (salinity) at the glider locations for RU05 is 0.275 degree (0.15 psu), for RU21 is 0.22 degree (0.13 psu) and for RU23 is 0.225 degree (0.12 psu). Most of the gliders collected data within 25–30 m depth, while the maximum depth of a particular glider was 63 m.

4. Analysis of post-assimilation fields in forecast mode

This section describes the assimilative forecasts and their analyses in understanding the impact of assimilation from a spatial and temporal footprint perspective.

4.1. Description of assimilative forecasts

The effect of the glider data assimilation on the forecasts is presented next (Figs. 10 –18). In the SMAST-HOPS assimilation strategy, in which glider data is assimilated every 12 h, objectively analyzed fields with appropriate error fields are first computed. The multiscale OA uses the data in the observational window of ± 12 h, and uses the initial field of Nov 2 as the background. This choice of background avoids discontinuities between glider data and climatological background.

Two parallel runs were carried out. Both runs were initialized with the FORMS methodology (SG12). Furthermore, glider data for the initial period of October 26 through Nov 1 were objectively analyzed with the FORMS-derived temperature and salinity fields to produce the reanalysis initial field. The first run was then carried out with satellite-derived SST assimilation only during the first 12 h of simulation for Nov 2 and then continued without further assimilation of glider data (temperature and salinity). This run is designated as "Run1." This run can be described as a run with assimilation of the glider data at initialization.

Another run was done with successive assimilation of temperature and salinity data from gliders RU05, RU21 and RU23.

Please cite this article as: Gangopadhyay, A., et al., Multiscale forecasting in the western North Atlantic: Sensitivity of model forecast skill to glider data assimilation. Continental Shelf Research (2012), http://dx.doi.org/10.1016/j.csr.2012.09.013

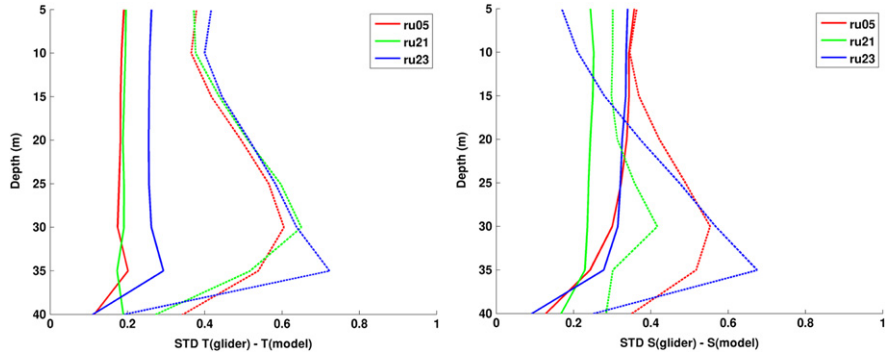

Fig. 6. Glider-OA error at various depths for (left) temperature and (right) salinity. The abscissa is the standard deviation of the difference between the glider data and the OA fields every 12 h.

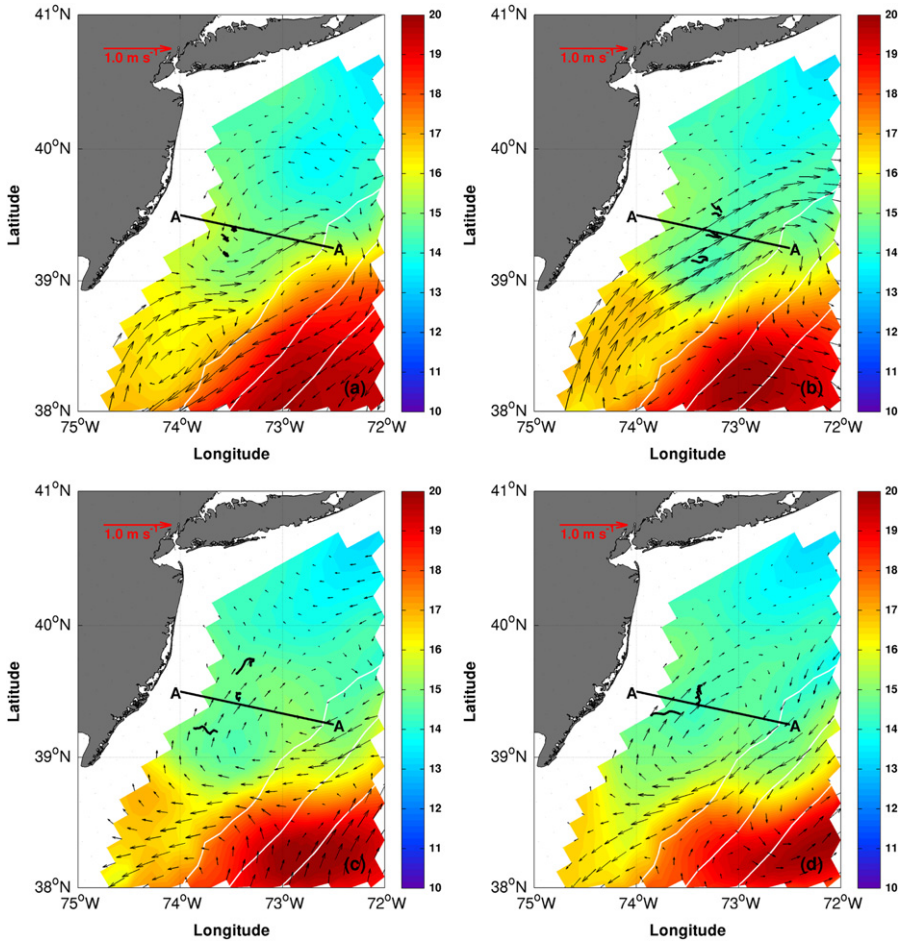

Fig. 7. Twenty-five metre temperature and velocity vectors from 02 Nov 2009 run for (a) 03 Nov 2009, (b) 05 Nov 2009, (c) 07 Nov 2009, and (d) 09 Nov 2009. Solid line A–A shows cross-section region and thick black squiggles show glider positions for data that is assimilated for each day. Temperature in °C.

The satellite-derived SST assimilation methodology is very similar to that described by SG12. Additionally, glider data was assimilated following the methodology described in Section 3. This run is designated as "Run2." Following SG12, the initial field was adjusted for SST assimilation on the first cycle (12 h), which also assimilated the temperature and salinity from the gliders between Oct 26 and Nov 2. The evolution of temperature at 25 m overlaid with velocity for the assimilation run (Run2) for the first week is presented in Fig. 7. The evolution of salinity at 25 m overlaid with velocity for the second week is shown in Fig. 8. The initially weak velocity field develops and adjusts to about 0.1 m s^{-1} of southwestward flow along the shelf between the 50- and 100-m isobaths, while an anticyclonic recirculation develops between 38°N and 39°N (not shown). The weak southward flow to the north of the glider confluence region (Fig. 7) dissipates by Nov 3–5, when a broad northwestward wind-induced flow occurs over the glider region (not shown). During Nov 5–7, the passage of a southwesterly storm was reported. The expansion of glider data assimilation is greatest (in terms of areal coverage) on Nov 7 (Fig. 7). The velocity field adjusts to an

Please cite this article as: Gangopadhyay, A., et al., Multiscale forecasting in the western North Atlantic: Sensitivity of model forecast skill to glider data assimilation. Continental Shelf Research (2012), http://dx.doi.org/10.1016/j.csr.2012.09.013

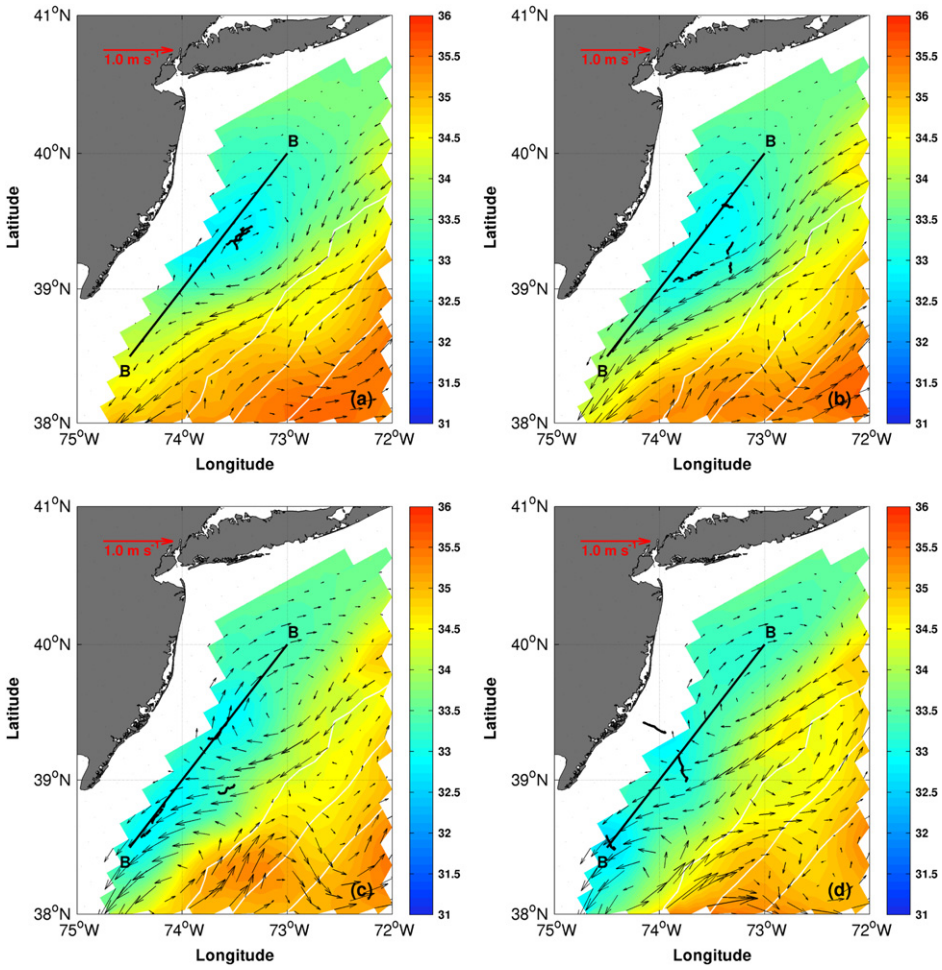

Fig. 8. Twenty-five metre salinity and velocity vectors from 02 Nov 2009 run for (top left) 10 Nov 2009, (top right) 12 Nov 2009, (bottom left) 14 Nov 2009, and (bottom right) 16 Nov 2009. Solid line B–B shows cross-section region, and thick black squiggles show glider positions for data that is assimilated for each day.

anticyclonic eddy-like shelf feature over the glider region (Fig. 7) by Nov 9 to the north of the steady southwestward along-shelf flow.

Fig. 9 shows a sectional view along line AA (Fig. 7) of the evolution of salinity during Nov 3–9. The initial shelf field is dominated by a shallow patch of relatively fresh water (S∼32–33 psu) (Fig. 9a). The contrast between this patch of fresh water and the higher-salinity water from climatological fields creates the salinity front (33–34 psu) between 60 km and 80 km offshore. Most of the glider data assimilated during Nov 3–5 has a uniform vertical profile. As assimilation progressively captures the low-salinity data, the frontal boundary between the near-coastal fresh water and offshore saline water moves gradually offshore and becomes tighter. The salinity front is visible between 80 km and 100 km offshore on Nov 5 and stabilizes at this location (Fig. 9b). The dynamical model shows further relative freshening of the offshore isohalines between 100 km and 150 km offshore during the latter part (Nov 7 through Nov 9) of the simulation (Fig. 9c and d). Note that the Jenifer Clark satellite analysis shows a possible intrusion around an anticyclonic shelf eddy near the glider assimilation region on Nov 6 (Fig. 10). However, in the dynamical model, the eddy was non-existence, as the model was initialized with the canonical shelf-slope front in this region. Thus the climatological signature of the shelf-slope front competes against the freshening and cooling induced by the assimilation of glider observations. Effectively, in the shallow inshore region, the dynamical model develops a weak signature of a fresher and cooler patch on the shelf. Had there been more observations around this area, one would then expect to capture dynamical events like "overrunning" (Kumar et al., 2006), which are deeper and closer to shelf-break.

The evolution of temperature during the week of Nov 2–9 is examined next (Fig. 11a–d) along the cross-shelf section indicated in Fig. 7. Since the SST from satellite images is also assimilated with a vertical projection algorithm, initial contrast between the cooler shelf and warmer offshore water decays rapidly. By day 3 of the assimilation, the temperature range on the shelf (<50 m) reduces to 14–15.3 °C (Fig. 14b and c) from the initial range of 14–16.5 °C (Fig. 11a). The signature of a significant front at about 150–200 km offshore (Fig. 11a) dissipates by day 3.

The weak signature of shelf water intrusion (evident in observation as shown in Fig. 10) across the shelf-break into the slope sea is visible in the temperature field by day 6 and also evident in the day-7 forecast at 60 km offshore (Fig. 11). The center of the simulated anomalous patch is cooler (14.1 °C) than its edges (14.7 °C) (Fig. 11d) at the surface. The patch is also fresher at the core, and the inshore salinity gradient is weaker than its offshore counterpart.

The impact of temperature and salinity assimilation of glider data during the first week is examined next (Figs. 12 and 13) along the north-south section (line *B* of Fig. 8). In the salinity section (Fig. 13a), the far-field impact of assimilation of the three drifters (RU05, RU21 and RU23) is evident in the fresh water signature near the middle of the section, bounded by the

Please cite this article as: Gangopadhyay, A., et al., Multiscale forecasting in the western North Atlantic: Sensitivity of model forecast skill to glider data assimilation. Continental Shelf Research (2012), http://dx.doi.org/10.1016/j.csr.2012.09.013

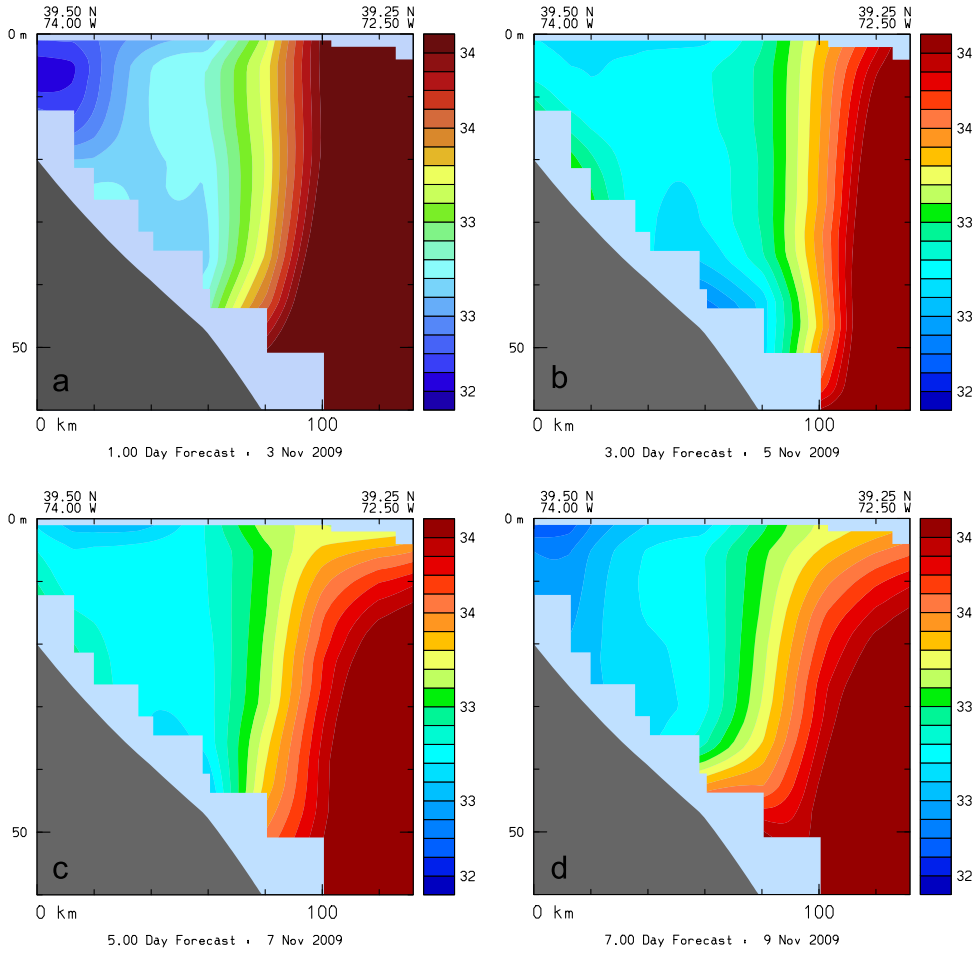

Fig. 9. Salinity cross sectional view of shelf along section line A–A, shown in Fig. 10 for 02 Nov 2009 SMAST-HOPS run with glider assimilation. Panels valid for (a) 03 Nov 2009, (b) 05 Nov 2009, (c) 07 Nov 2009, and (d) 09 Nov 2009.

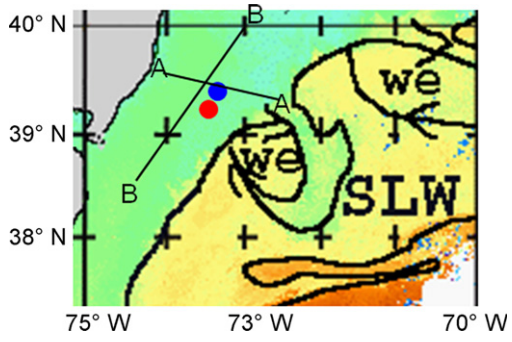

Fig. 10. Possible intrusion of shelf water into the slope during the OSE period. The image analysis is for Nov 6, 2009. Location of glider RU05 (RU23) is shown by the blue (red) dot in upper panel for Nov 6, 2009. The two sectional lines, A–A from Fig. 10, and B–B from Fig. 11, are also shown. (For interpretation of the references to color in this figure legend, the reader is referred to the web version of this article.)

climatological high-salinity patches. During the first week of the assimilation, the three gliders progressively sample the waters near and along this section, and the waters become fresher and colder due to assimilation. The vertical homogeneity of this assimilated water mass is strikingly different when compared to the unassimilated fields (not shown), which are generally more saline and warmer.

Further evolution of temperature and salinity along the north-south section (shown as B–B in Fig. 8) for the second week is shown in Figs. 14 and 15. This section follows the glider tracks of RU05 and UD134 during the second week of the OSE. Note that while the data from RU05 was assimilated into the model, the data from UD134 was used only for comparing the assimilated model results as an independent validation. The initial high-salinity patches are replaced by realistic fresher water on the shelf through subsequent glider data assimilation within the first week.

The weak signature of the shelf water intrusion across the shelf-break into the slope water, as discussed earlier, is also captured in the forecast fields of temperature (Fig. 14) and salinity (Fig. 15) of day 8 km, 100 km south of the northern end of the section. The subsurface saltier waters to the north and south are due to recirculation generated by the dynamical simulation.

4.2. Time-series comparison of Simulations against glider data

Fig. 16 shows a comparison of time-series of temperature and salinity of the assimilated reanalysis against the three gliders at 25 m. The simulated temperature and salinity profiles of the data-assimilative model are compared with the actual glider profiles at glider locations every half-hour. The assimilation evidently captures the inertial and sub-inertial variability reasonably well (Fig. 16). Difference in the initial 1–2 days between the assimilated simulation and glider data can be attributed to the possible mismatch between the satellite-derived SST (and its extrapolation

Please cite this article as: Gangopadhyay, A., et al., Multiscale forecasting in the western North Atlantic: Sensitivity of model forecast skill to glider data assimilation. Continental Shelf Research (2012), http://dx.doi.org/10.1016/j.csr.2012.09.013

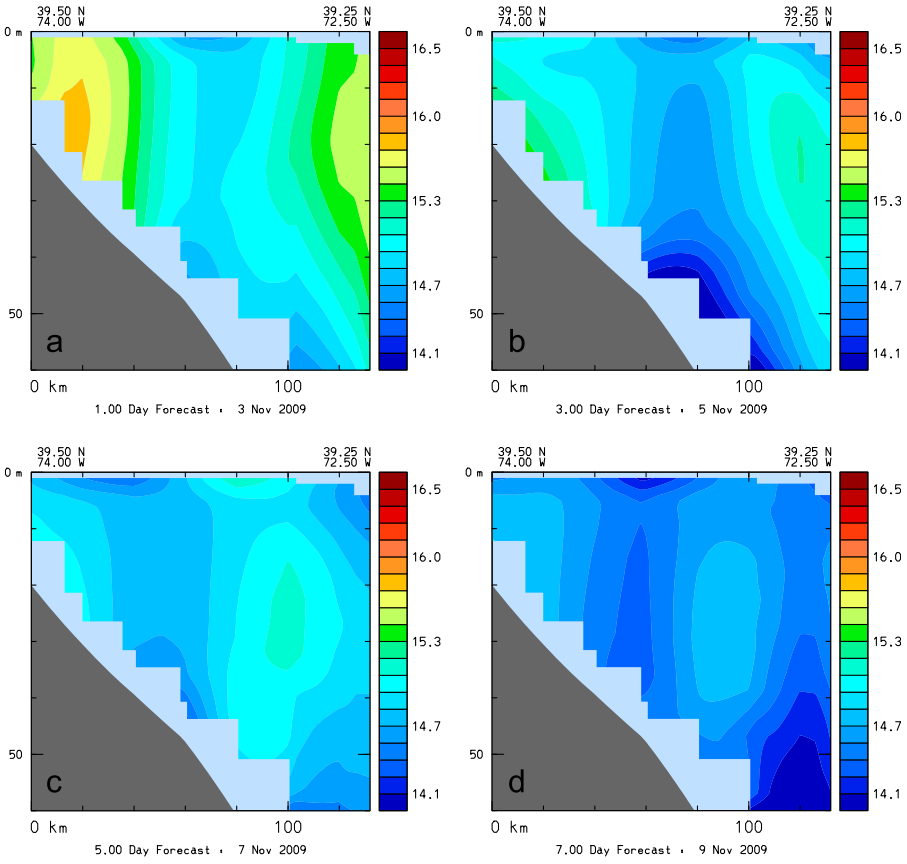

Fig. 11. Temperature cross sectional view of shelf along section line A–A, shown in Fig. 10 for 02 Nov 2009 SMAST-HOPS run with glider assimilation. Panels valid for (a) 03 Nov 2009, (b) 05 Nov 2009, (c) 07 Nov 2009, and (d) 09 Nov 2009.

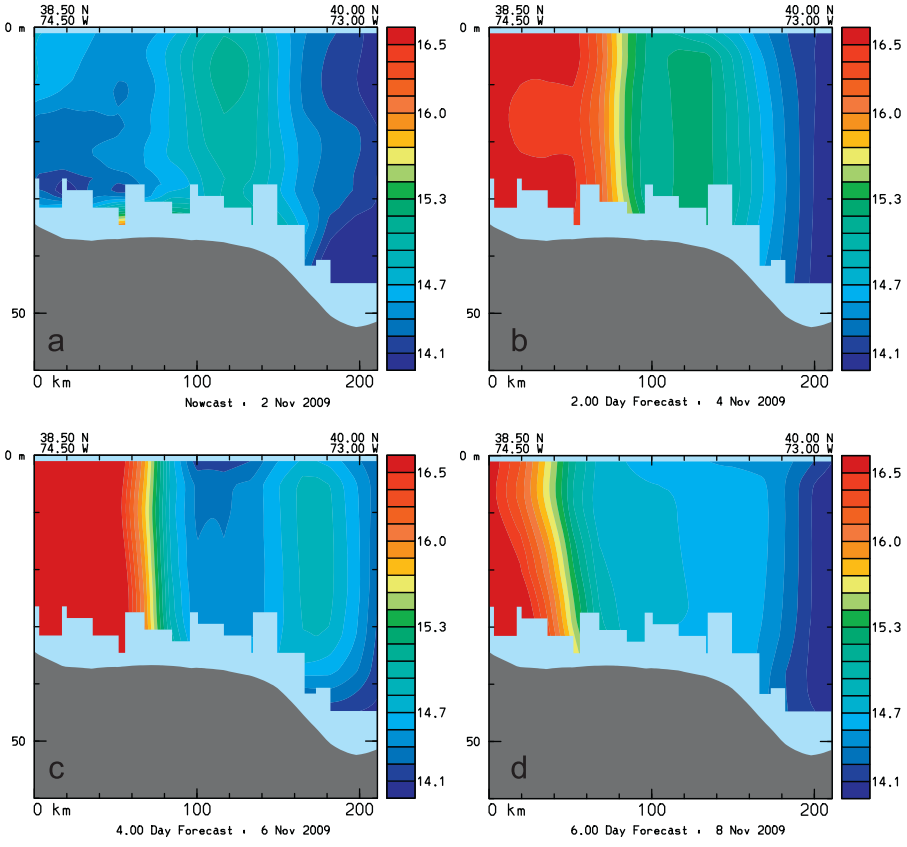

Fig. 12. Temperature cross sectional view of shelf along section line B–B, shown in Fig. 11 for 02 Nov 2009 SMAST-HOPS run with glider assimilation. Panels valid for (a) 02 Nov 2009, (b) 04 Nov 2009, (c) 06 Nov 2009, and (d) 09 Nov 2009.

Please cite this article as: Gangopadhyay, A., et al., Multiscale forecasting in the western North Atlantic: Sensitivity of model forecast skill to glider data assimilation. Continental Shelf Research (2012), http://dx.doi.org/10.1016/j.csr.2012.09.013

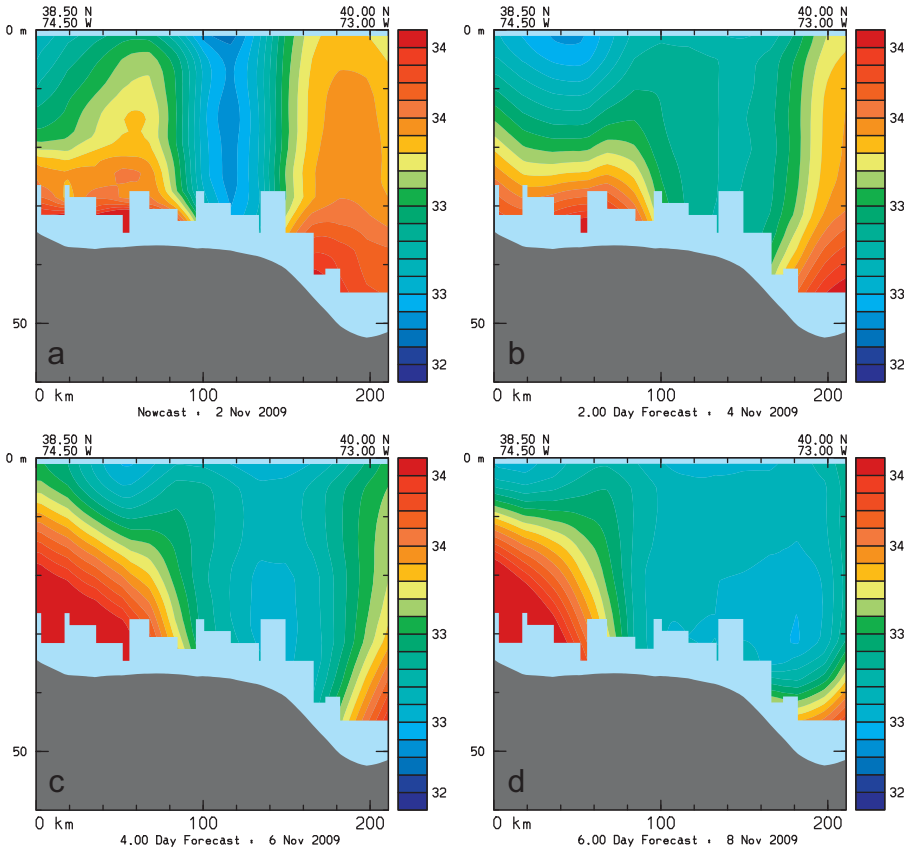

Fig. 13. Salinity cross sectional view of shelf along section line B–B, shown in Fig. 11 for 02 Nov 2009 SMAST-HOPS run with glider assimilation. Panels valid for (a) 02 Nov 2009, (b) 04 Nov 2009, (c) 06 Nov 2009, and (d) 09 Nov 2009.

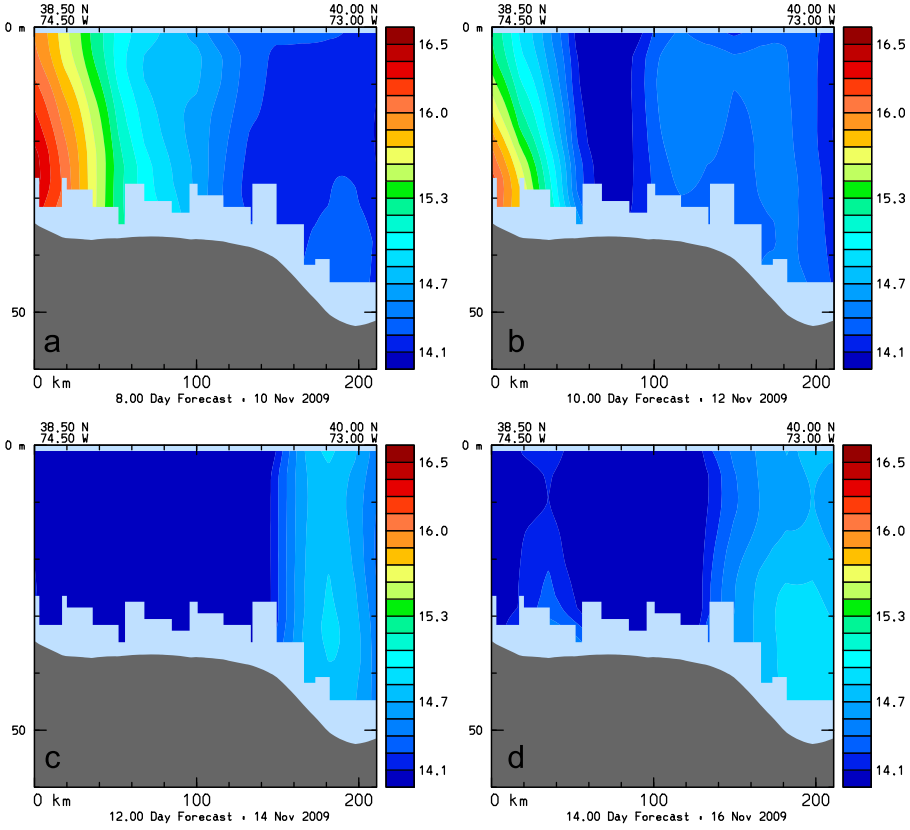

Fig. 14. Temperature cross sectional view of shelf along section line B–B, shown in Fig. 11 for 02 Nov 2009 SMAST-HOPS run with glider assimilation. Panels valid for (a) 10 Nov 2009, (b) 12 Nov 2009, (c) 14 Nov 2009, and (d) 16 Nov 2009.

Please cite this article as: Gangopadhyay, A., et al., Multiscale forecasting in the western North Atlantic: Sensitivity of model forecast skill to glider data assimilation. Continental Shelf Research (2012), http://dx.doi.org/10.1016/j.csr.2012.09.013

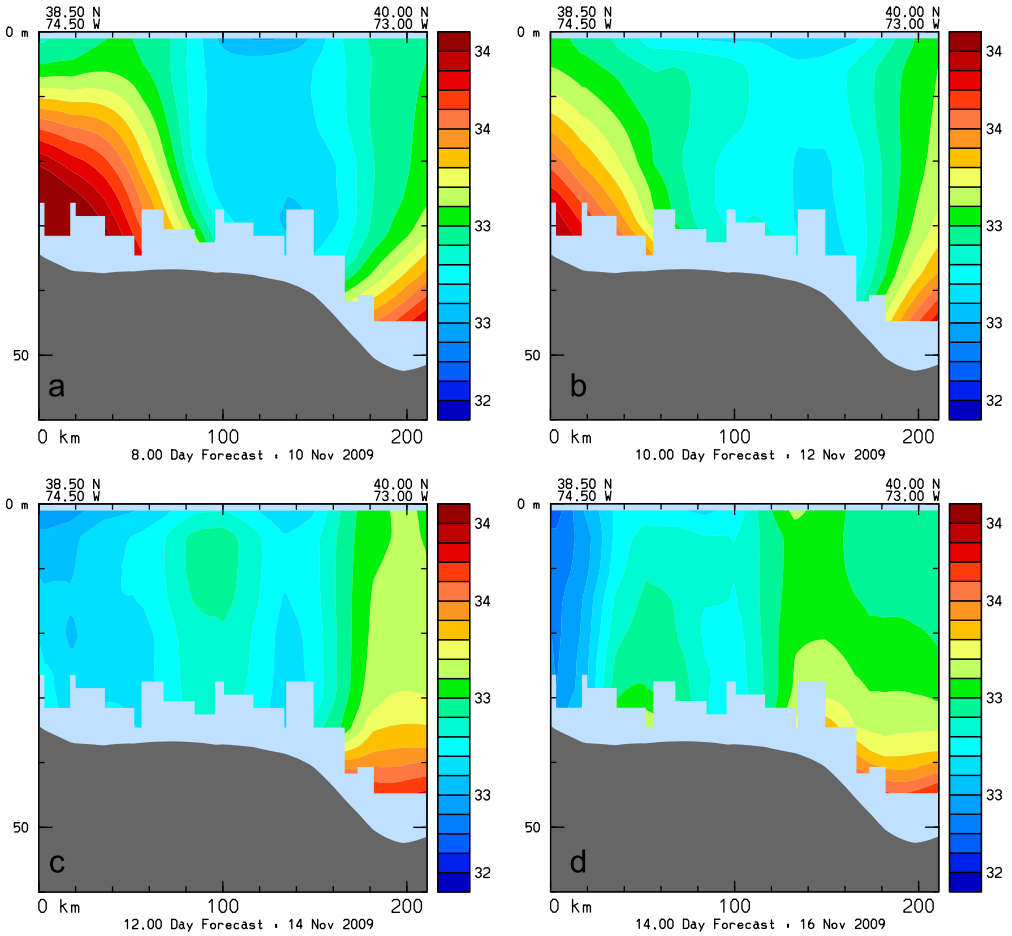

Fig. 15. Salinity cross sectional view of shelf along section line B–B, shown in Fig. 11 for 02 Nov 2009 SMAST-HOPS run with glider assimilation. Panels valid for (a) 10 Nov 2009, (b) 12 Nov 2009, (c) 14 Nov 2009, and (d) 16 Nov 2009.

to depth with a mixed-layer-dependent formulation) and glider temperature (and its vertical uniformity in shallow waters).

Differences between assimilated salinity and glider data can be attributed to the initial mismatch of climatological average salinity with glider data. In all cases, the assimilated temperature and salinity tends to match with glider observations after this initial 1- to 2-day period of internal adjustment (Fig. 16).

Fig. 17 shows a time-series comparison of UD134 data against assimilated forecast at available locations as an independent measure of model skill. The comparison is shown for forecast days 6 and 7. Note that the large biases of the non-assimilated temperature and salinity from the climatology-based shelf initialized run are on the order of 2 °C and 1 psu, respectively. This comparison points to the need for glider assimilation for monitoring the shelf circulation in the Mid-Atlantic Bight region.

The rms differences between the assimilated and non-assimilated runs and the glider data for various depths are shown in Fig. 18. It is apparent that the errors are depth-independent after assimilation. This is probably an artifact of most of the glider data being vertically uniform. However, the depth variation of the unassimilated differences indicates the possibility of assimilation having a bigger impact in the subsurface than at the surface due to glider data. This might be due to the lesser variability at depth than at surface, accentuating the impact of assimilation in the subsurface fields.

However, there are two other ways the glider data could show more impact on the subsurface than on the surface. The first is that SST is being assimilated prior to glider data assimilation, which should make the surface temperature in the model move closer to the glider observation at the surface, leaving the subsurface temperature un-corrected. Thus, the impact of temperature assimilation may seem larger after correction at subsurface (although, not so for salinity correction). Second, the observed Glider profiles for November 2009 depicts a well-mixed, almost-constant profile of temperature and salinity, while the cliamtological profiles at these locations, which the model used for initialization had stratification, aka, more subsurface variability. So, after assimilation, the subsurface impact seems larger than that at the surface.

Furthermore, averaged over the two-day (Nov 8–10) time period, the salinity difference between assimilated and non-assimilated runs is about 0.5 psu (Fig. 17b), while the temperature deviation is about 2 °C (Fig. 17a). Since the salinity difference is comparable to the range of assimilation rms (Fig. 18b) of 0.4 ppt, while the SST difference of 2 °C is an order of magnitude higher than the temperature assimilation rms (0.2 °C, Fig. 18a), it is conceivable that salinity assimilation might affect the water column for a longer time period.

4.3. On the temporal and spatial decay of the assimilation footprint

The nature of the decay of the impact of temperature and salinity assimilation is examined next. To determine the temporal decay footprint, we chose two assimilation locations, one offshore (O) and another inshore (I). The OA contours of assimilation errors are presented in Fig. 19a and b, for Nov 6th and 10th, which show the coverage of assimilation for those respective dates. These two locations allowed for tracking the temperature and salinity decay

Please cite this article as: Gangopadhyay, A., et al., Multiscale forecasting in the western North Atlantic: Sensitivity of model forecast skill to glider data assimilation. Continental Shelf Research (2012), http://dx.doi.org/10.1016/j.csr.2012.09.013

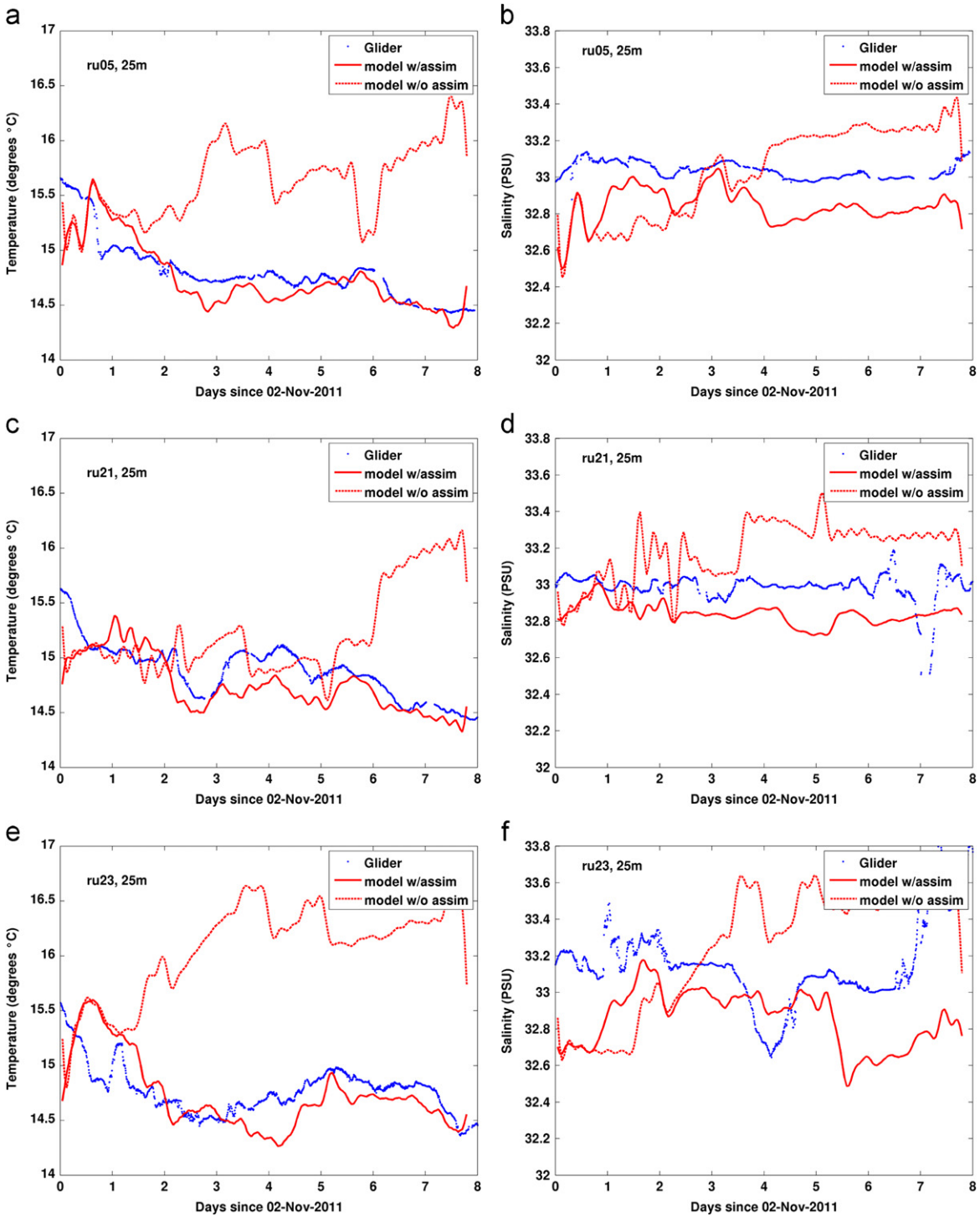

Fig. 16. Twenty-five metre time series of glider (left) temperature and (right) salinity for gliders ((a) and (b)) RU05, ((c) and (d)) RU21, and ((e) and (f)) RU23, compared to the SMAST-HOPS 02 Nov 2009 runs. Glider data are shown with blue dots, the model run with glider assimilation is shown with a solid line, and the model run with no glider assimilation is shown with a dashed line. Temperature in °C, salinity in psu.

scales after the peak of assimilation (marked by arrows in the figures on the error time-series) on Nov 8th for point I (Fig. 19c and e) and after Nov 6th for point O (Fig. 19d and f).

Effectively, there was a single assimilation window of about 2 days for I (Nov 6–8); while for point O, there were two assimilation windows: one for about two days (Nov 4–6) and another also for a different two days (Nov 12–14) at the end of the reanalysis period. The assimilation of satellite-derived SST during the first 12 h, and the ingestion of available glider data at initialization, induced similar impact up to about 0.75 day to both unassimilated and assimilated simulations (Fig. 19c–f). The assimilation during Nov 4–6 then corrects the developing forecast, while the unassimilated forecast behaves differently. After this initial phase, the assimilated temperature takes about

Please cite this article as: Gangopadhyay, A., et al., Multiscale forecasting in the western North Atlantic: Sensitivity of model forecast skill to glider data assimilation. Continental Shelf Research (2012), http://dx.doi.org/10.1016/j.csr.2012.09.013

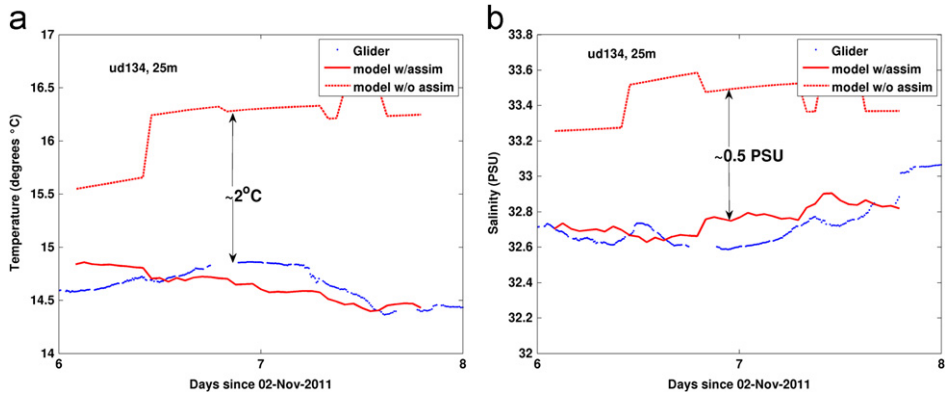

Fig. 17. Twenty-five metre time series of glider UD134 (a) temperature and (b) salinity, compared to the SMAST-HOPS 02 Nov 2009 runs. Glider data are shown with blue dots, the model run with glider assimilation is shown with a solid line, and the model run with no glider assimilation is shown with a dashed line. Temperature in °C, salinity in psu. Note the difference between assimilation and non-assimilation runs for temperature is about 2 °C; while that for salinity is about 0.5 psu.

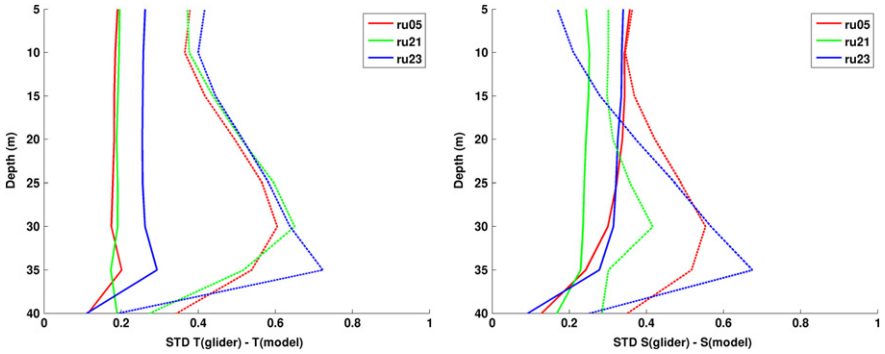

Fig. 18. Glider-model error at various depths for (left) temperature and (right) salinity. The abscissa is the standard deviation of the difference between the glider and the model. The solid lines represent differences between the gliders and the model run with glider assimilation; the dashed lines represent differences between the gliders and the model run with no assimilation. For both types of model runs, the gliders were used for the initial field.

1–2 days to degrade to the levels of non-assimilated run, while salinity takes 3–4 days for point I and about 2 days for point O. The temperature decay time-scales are similar to those (1–1.5 days) obtained for Monterey Bay by Shulman et al. (2009).

Two interesting results are clear from Fig. 19. First, after the assimilation is over, the salinity tends to approach back to the unassimilated value in time, while the temperature settles to a new threshold level and follows the behavior of the unassimilated temperature simulation. Second, the larger the difference between the unassimilated simulation and observation (at the beginning of the assimilation), the longer it takes for the tracer to approach the unassimilated behavior and/or the value itself. Note that we also found these two results to be depth-independent.

The spatial scales of decay for the impact of assimilation are investigated next. Three points (South—S; Middle—M; and North—N) were chosen along one transect through the glider array (Fig. 2) for the spatial decay experiment. The daily difference in temperature field between the runs with and without assimilation is presented in Fig. 20a. Greater difference at the time of assimilation indicates greater impact. Persistence of the initial difference over time beyond the point at which assimilation is discontinued would imply a prolonged impact of assimilation. It is clear from Fig. 20a that the temperature impact decays significantly within the first 2–4 days for all points (S, M, and N), and that the amplitude of the impact decreases with distance from the glider location (point of assimilation). The salinity impact does not show such drastic decay (Fig. 20c) at these locations. The spatial decay scale for the temperature is obtained from Fig. 20a, where the difference in temperature (assimilation vs. non-assimilation) is examined as a function of distance from the assimilation location for two consecutive days (days 3 and 4) after the assimilation is over on day 1.

The exponential nature of the spatial decay of temperature impact from the center of assimilation outward is evident for all days (other days not shown). The e-folding impact scale is determined to be about 100 km for the third day, and about 60 km for the fourth day. In contrast, the salinity signal does not show any preferential decay pattern (Fig. 20d). The salinity difference fluctuates within a narrow range around the initial difference for day 3, and stays almost same for day 4. No consistence spatial-decay pattern for salinity was found in these three locations.

The above differences in the temperature and salinity behavior beget the idea of using different decorrelation parameters for objective analysis of temperature and salt information for assimilation. For example, different decorrelation scales for temperature and salinity error covariance computation were used (Reinicker et al., 2011) by the Global Modeling and Assimilation Office (GMAO) at the NASA/Goddard Space Flight Center for ocean initialization for seasonal-to-interannual climate prediction efforts (http://gmao.gsfc.nasa.gov/research/ocean; Keppenne et al., 2005; Sun et al., 2007). Typically, temperature decorrelation scales (20° zonal, 8° meridional and 100 m in the vertical) are larger than those for salinity (8° zonal, 3° meridional and 40 m in the vertical). Our results indicate similar

Please cite this article as: Gangopadhyay, A., et al., Multiscale forecasting in the western North Atlantic: Sensitivity of model forecast skill to glider data assimilation. Continental Shelf Research (2012), http://dx.doi.org/10.1016/j.csr.2012.09.013

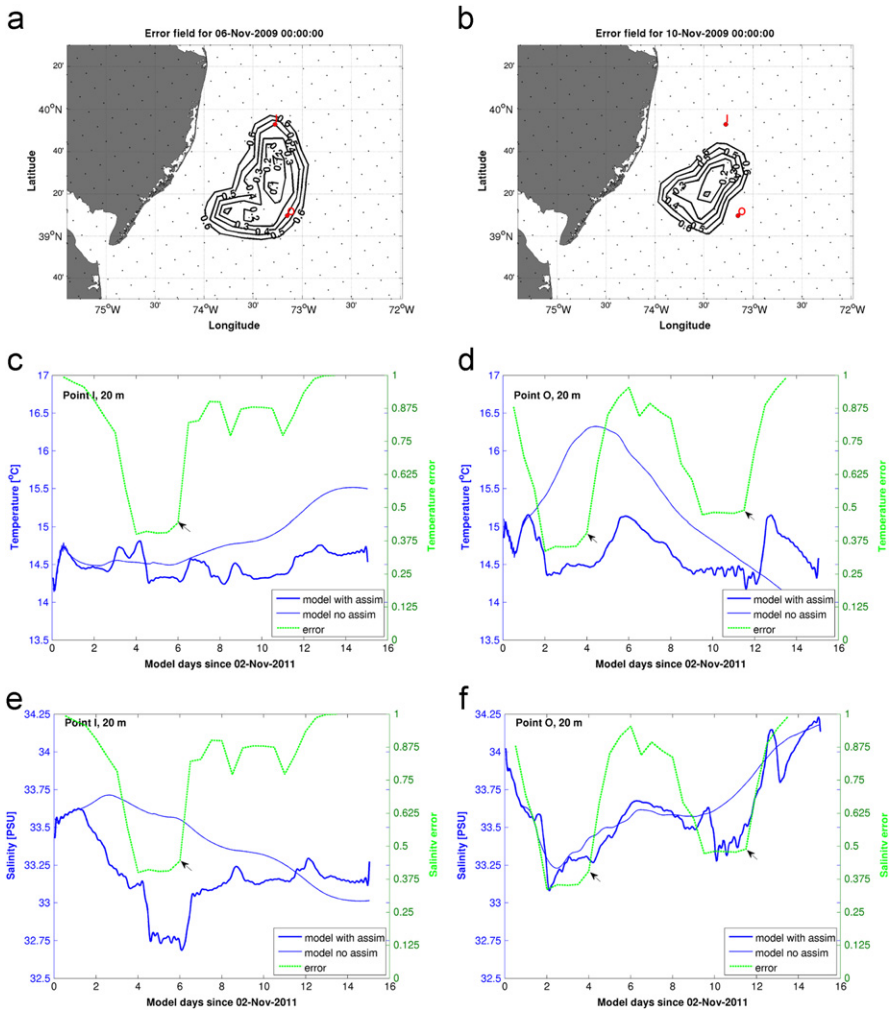

Fig. 19. Temporal behavior of temperature and salinity after assimilation. The error maps of OA fields (T, S) are shown for 4th Nov in (a) and for 10th Nov in (b). The simulation time-series with and without assimilation are shown for temperature at point I and point O are shown in the middle panels ((c) and (d)). Superimposed is the time-series of the error at these locations in dash-line. Similarly, the bottom panels show the salinity fields at these locations. The black arrow in the middle and bottom panels identifies the end of the assimilation period at each location.

qualitative differences in spatial impact of assimilation between temperature and salinity might also exist in the shelf region, albeit at a finer-scale (10s of kilometers for the shelf as opposed to 100s of kilometers for the global models).

5. Summary and discussion

This study presented an application of the SMAST-HOPS real-time forecast system developed for the western North Atlantic during the OOI–CI OSE period (Oct 26–Nov 17, 2009). The ring and front analysis from satellite imagery is used to feed into the feature modeling scheme for generating a three-dimensional initial field. The initialization field is dynamically adjusted with wind-forcing and used in an SST-glider-assimilative (temperature- and salinity-assimilative) forecast model. The model was forced by atmospheric fields from the global forecast system in real time. The forecast fields were made available via a THREDDS data server for easy and efficient extraction by scientists and application developers for glider planning, control and guidance.

The feature-based initialization scheme was utilized for 4 short-term forecasts of varying lengths during the first two weeks of November 2009 in an ensemble mode with other forecasts to guide glider control. A reanalysis was then carried out, assimilating the data from three gliders (RU05, RU21 and RU23) for the two-week period. Results are first compared against data from these three gliders, and then against the independent data from the other glider, UD134. Results from the assimilation are also analyzed to evaluate the impact of glider data and sensitivity of model forecasts to data assimilation. The assimilation of salinity improved the model performance in the area around the data and impacted the subsurface fields. An interesting result was that assimilating (or infusing) the available glider data at initialization enabled the model to smoothly absorb and adjust subsequent cycles of assimilation of patchy glider data.

The glider data assimilation led to a depth-averaged model-data difference of 2 °C for temperature and 0.5 psu for salinity for the upper 25 m of the Mid-Atlantic shelf. A sensitivity analysis was carried out to determine the short-term memory of the simulated ocean. The forecast fields retained assimilated temperature information for about 1–2 days. No coherent pattern for temporal decay of salinity was determined with its range varying from 1–4 days at different locations. However, significant differences in their patterns of behavior after assimilation were clearly observed.

It is interesting to note that the short-term retention period (of temperature and salinity impact) might be increased by

Please cite this article as: Gangopadhyay, A., et al., Multiscale forecasting in the western North Atlantic: Sensitivity of model forecast skill to glider data assimilation. Continental Shelf Research (2012), http://dx.doi.org/10.1016/j.csr.2012.09.013

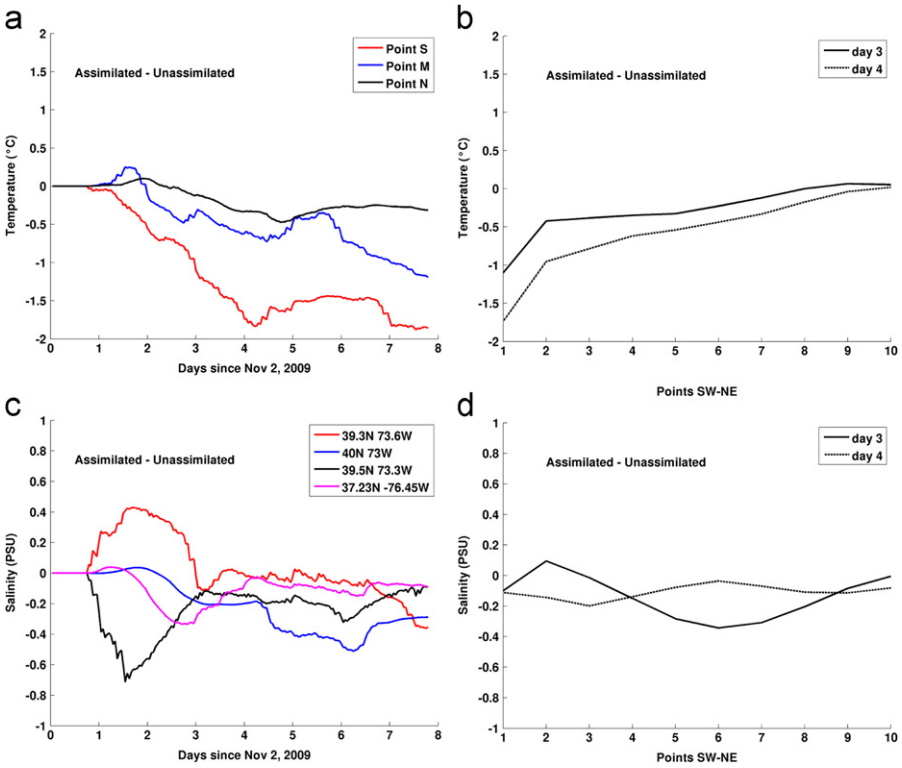

Fig. 20. (a) The temperature difference between the runs with and without assimilation at the three locations (S, M and N) as time progresses after assimilation on Nov 02, 2009 at point S; (b) the temperature difference for days 3 and 4 away from the assimilation point S as shown in Fig. 5; (c) similar to (a), but for salinity; (d) similar to (b), but for salinity.

increasing the model resolution in the horizontal and vertical. While increasing the resolution will result in resolving more features (effectively adding more wave numbers and reducing the de-correlation scales); the underlying OI assimilation scheme brings high-resolution assimilation (correction) fields, because the observations are mapped on the model grid prior to assimilation. Such sensitivity/competition studies would be carried out in future studies. Our results on temporal decay (1–3 days) of temperature after assimilation are consistent with those (1–1.5 days) found by Shulman et al. (2009) for the Monterey Bay region.

It is intriguing to also note that one would expect a sizeable difference in the decay scales of temperature and salinity linked to the underlying real (molecular) diffusivity of the variables. In reality, the short-term temporal memory of the ocean could be thought to be inversely proportional to the diffusivity of the tracer. For example, due to its slower diffusivity, the retention period of assimilated salinity signature may be longer than that of the temperature. Similarly, the spatial footprint of the impact could be directly proportional to the diffusivity. Consequently, the spatial decay scale for assimilated temperature would be larger than that of the assimilated salinity signal (consistent with Reinicker et al. 2010 for GMOA). However, most of the dynamical models (including the present one used here) employ the same numerical diffusivity for the prognostic runs, which might or might not be appropriate for both tracers. More sensitivity experiments would be necessary to further quantify and understand such differences between the temperature and salinity response after assimilation.

The impact analyses presented before clearly shows that there exists certain differences in the spatial and temporal influence windows (scales, footprints) after assimilation for the two tracers, temperature and salinity. These new results open up the possibility of developing new assimilation algorithms which might be similar to the new developments of the EnKF, where variables maintaining two different scales are assimilated in a combined scheme (Ballabrera-Poy et al., 2009). The ideas of scale-preserving assimilation (Lorenc, 2003; Kalnay et al., 2007) and of 'variable localization' for constructing covariance matrix in EnKF (Kang et al., 2011) seem worth investigating in this context of multiple tracers. Specifically, temperature and salinity could be the oceanic proxies for the temperature and carbon (and/or humidity) in the atmospheric models and these new assimilation techniques.

These differences in impact of assimilation of temperature and salinity data and their possible link to the real-ocean diffusion of heat and salt also points to another area of research. Typical large-scale models (Navy's coastal ocean model, hybrid co-ordinate ocean model, regional ocean modeling system, modular ocean model, etc.) use the same diffusivity for both tracers for most applications. Systematic studies with different diffusivities for different tracers in regional modeling exercises in coastal regions such as the Mid-Atlantic shelf might lead to better understanding of processes and better forecasting capabilities for the many operational observing systems.

Based on the sensitivity analysis, a phased-assimilation strategy to assimilate both satellite SST and glider data with different weighting functions for temperature and salinity can probably be developed. For example, while 2-day composite satellite-derived SST fields can be assimilated every two days, individual glider data could be assimilated every day with a 12-h weighting function. However, if salinity data can be retained by the simulated ocean for a longer period of time, independent salinity observations, or satellite-derived chlorophyll-inferred seas surface salinity can be assimilated with different weighting function (yet-to-be-determined) on a different assimilation cycle. Another example would be of designing a phased observation-assimilation scheme, in which XBT

Please cite this article as: Gangopadhyay, A., et al., Multiscale forecasting in the western North Atlantic: Sensitivity of model forecast skill to glider data assimilation. Continental Shelf Research (2012), http://dx.doi.org/10.1016/j.csr.2012.09.013

observations will be assimilated frequently to supplement SST fields to realize the subsurface thermal structure, while XCTD observations will be sampled and assimilated more sparsely to match and allow for larger retention period of salinity. In the near future, such a system of "phased assimilation" of satellite SST, sea surface color (SSC), glider data and other in-situ observations could be built for monitoring the changes of the water masses in the Mid-Atlantic more efficiently, economically, and knowledgeably.

Acknowledgements

This real-time forecast system has been made possible due to many years of research at Harvard University, UMass Dartmouth, MIT and other institutions by many researchers. We appreciate all of their past efforts and current support. Special thanks are due to our colleagues at MIT who are supporting our efforts with the software and analysis packages. Funding was made available from the Office of Naval Research (ONR) MURI program (N000140610739), the National Aeronautics and Space Administration (NASA), the National Oceanic and Atmospheric Administration (NOAA) and the National Science Foundation (NSF) at different times to different PIs at different institutions. We acknowledge all their efforts and support. Current funding from NOAA under IOOS for MARACOOS and the support of the MACOORA group are gratefully acknowledged. We appreciate the efforts of Applied Science Associates and the Rutgers group for making the glider data available in a format for easy analysis. Our special thanks to Dr. Wendell Brown for his insight in implementing an earlier version of the model system and many discussions in-house on the OSE–Glider-modeling exercises. We appreciate the help, support and guidance of Drs. Scott Glenn, Bill Boicort and the entire MARACOOS group during the OSE. Special thanks to John Kerfoot for his work in making the glider data available in real-time. We thank the other five modeling teams from Rutgers (John Wilkin and his group), Stevens (Alan Blumberg and his group), JPL (Yi Chao and his group), MIT (Pierre Lermusiaux and his group) and USGS (Rich Signell, John Warner and their group), with whom we participated in the OSE real-time ensemble exercises. We wish to acknowledge the invaluable experience gathered during the OOI–CI–OSE on the infrastructure issues of real-time forecasting from the interactions with the JPL, UCSD and the larger CI team. We are appreciative of the help provided by Mr. Frank Smith at SMAST with editing this manuscript.

Our sincere thanks to the reviewers and the editors of this special issue for their comments, patience and support during the revision of this manuscript, which helped clarify many details.

References

Ballabrera-Poy, J., Kalnay, E., Yang, S., 2009. Data assimilation in a system with two scales-combining two initialization techniques. Tellus 61A, 539–549.

Barrick, D.E., 1972. First-order theory and analysis of mf/hf/vhf scatter from the sea. IEEE Transactions on Antennas and Propagation AP-20, 2–10.

Barrick, D.E., Evens, M.W., Weber, B.L., 1977. Ocean surface currents mapped by radar. Science 198, 138–144.

Barron, C.N., Smedstad, L.F., Dastugue, J.M., Smedstad, O.M., 2007. Evaluation of ocean models using observed and simulated drifter trajectories: Impact of sea surface height on synthetic profiles for data assimilation. Journal of Geophysical Research 112, C07019, http://dx.doi.org/10.1029/2206JC003982.

Bhushan, S., Blumberg, A.F., Georgas, N., 2009. "Comparison of NYHOPS hydrodynamic model SST predictions with satellite observations in the Hudson River tidal, estuarine, and coastal plume region", Eleventh International Conference in Estuarine and Coastal Modeling. ECM11, 4–6 November 2009, Seattle, WA. American Society of Civil Engineers, pp. 11–26.

Blackwell, S.H., Moline, M.A., Schaffner, A., Garrison, T., Chang, G., 2008. Sub-kilometer length scales in coastal waters. Continental Shelf Research 28 (2), 215–226.

Broquet, G., Edwards, C.A., Moore, A.M., Powell, B.S., Veneziani, M., Doyle, J.D., 2009. Application of 4D-Variational data assimilation to the California current system, dynamics of atmos. Oceans, http://dx.doi.org/10.1016/j.dynatmoce.2009.03.001.

Brown, W.S., Gangopadhyay, A., Bub, F.L., Yu, Z., Strout, G., Robinson, A.R., 2007a. An operational circulation modeling system for the Gulf of Maine/Georges Bank region, Part 1: The basic elements. IEEE Journal of Oceanic Engineering 32 (4), 807–822.

Brown, W.S., Gangopadhyay, A., Yu, Z., 2007b. An operational circulation modeling system for the Gulf of Maine/Georges Bank region, Part 2: Applications. IEEE Journal of Oceanic Engineering 32 (4), 823–838.

Calado, L., Gangopadhyay, A., da Silveira, I.C.A., 2008. Feature-oriented regional modeling and simulations (FORMS) for the western South Atlantic, south-eastern Brazil region. Ocean Modeling 25, 48–64.

Carter, E.F., Robinson, A.R., 1987. Analysis models for the estimation of oceanic fields. Journal of Atmospheric and Oceanic Technology 4 (1), 49–74.

Chao, Y., Li, Z., Farrara, J., McWilliams, J.C., Bellingham, J., Capet, X., Chavez, F., Choi, J.-K., Davis, R., Doyle, J., Fratantoni, D., Li, P., Marchesiello, P., Moline, M.A., Paduan, J., Ramp, S., 2009. Development, implementation, evaluation of a data-assimilative ocean forecasting system off the central California coast. Deep-Sea Research II, http://dx.doi.org/10.1016/j.dsr2.2008.08.011.

Crombie, D.D., 1955. Doppler spectrum of sea echo at 13.56 Mc/s. Nature 175, 681–682.

Davis, R.E., Webb, D.C., Regier, L.A., Dufour, J., 1992. The autonomous Lagrangian circulation explorer (ALACE). Journal of Atmospheric and Oceanic Technology 9, 264–285.

Derber, J.C., Rosati, A., 1992. A global ocean data assimilation system. Journal of Physical Oceanography 19, 1333–1347.

Eriksen, C.C., Osse, T.J., Light, R.D., Wen, T., Lehman, T.W., Sabin, P.L., Ballard, J.W., Chiodi, A.M., 2001. Seaglider: a long-range autonomous underwater vehicle for oceanographic research. IEEE Journal of Oceanic Engineering 26, 424–436.

Evensen, G., 2009. Data Assimilation: The Ensemble Kalman Filter. Springer-Verlag.

Ezer, T., Mellor, G.L., 1992. A numerical study of the variability and the separation of the Gulf Stream induced by surface atmospheric forcing and lateral boundary flows. Journal of Physical Oceanography 22, 660–682.

Fukumori, I., Malanotte-Rizzoli, P., 1995. An Approximate Kalman Filter for ocean data assimilation: an example with an idealized Gulf Stream model. Journal of Geophysical Research 100, 6777–6793.

Gangopadhyay, A., Lermusiaux, P.F.J., Rosenfeld, L.K., Robinson, A.R., Calado, L., Kim, H.S., Leslie, W.G., Haley Jr., P.J., 2011. California current system: a multiscale overview and the development of a feature-oriented regional modeling system (FORMS). Dynamics of Atmopsheres and Oceans 52 (1–2), 131–169, http://dx.doi.org/10.1016/j.dynatmoce.2011.04.003, Sept 2011.

Gangopadhyay, A., Robinson, A.R., 2002. Feature oriented regional modeling of oceanic fronts. Dynamics of Atmosphere and Oceans 36 (1–3), 201–232.

Gangopadhyay, A., Robinson, A.R., Arango, H.G., 1997. Circulation and dynamics of the western North Atlantic, I: Multi-scale feature models. Journal of Atmospheric and Oceanic Technology 14 (6), 1314–1332.

Gangopadhyay, A., Robinson, A.R., Haley Jr., P.J., Leslie, W.G., Lozano, C.J., Bisagni, J.J., Yu, Z., 2003. Feature oriented regional modeling and simulations (FORMS) in the Gulf of Maine and Georges Bank. Continental Shelf Research. 23 (3–4), 317–353.

Georgas N., Blumberg, A.F., 2009. "Establishing confidence in marine forecast systems: the design and skill assessment of the New York Harbor observation and prediction system, version 3 (NYHOPS v3)", Eleventh International Conference in Estuarine and Coastal Modeling. ECM11, 4–6 November 2009, Seattle, WA. American Society of Civil Engineers, pp. 660–685.

Glenn, S.M., Schofield, O., 2003. Observing the oceans from the COOLroom: our history, experience, and opinions. Oceanography 16 (4), 37–52.

Glenn, S., Schofield, O., 2009. Growing a distributed ocean observatory: our view from the COOL room. Oceanography 22 (2), 78–92.

Gould, J., Roemmich, D., Wijffels, S.H., Freeland, H., Ignaszewsky, M., Jianping, X., Pouliquen, S., Desaubies, Y., Send, U., Radhakrishand, K., Takeuchi, K., Kim, K., Danchenkov, M., Sutton, P., King, B., Owens, B., Riser, S., 2004. Argo profiling floats bring new era of in situ ocean observations. EOS 85 (19), 1136843, OI: 10.1126/science.

Haley Jr., P.J., Lermusiaux, P.F.J., 2010. Multiscale two-way embedding schemes for free-surface primitive-equations in the multidisciplinary simulation, estimation and assimilation system. Ocean Dynamics 60, 1497–1537, http://dx.doi.org/10.1007/s10236-010-0349-4.

Halpern, D.A., 2000. Satellites, Oceanography and Society. Elsevier Sci., Amsterdam, 361 pp.

Hayes, S.P., Mangum, L.J., Picaut, J., Sumi, A., Takeuchi, K., 1991. TOGA–TAO: a moored array for real-time measurements in the tropical pacific ocean. Bulletin of the American Meteorological Society 72, 340–347.

Hunt, B.R., Kalnay, E., Kostelich, E.J., Ott, E., Patil, D.J., Sauer, T., Szunyogh, I., Yorke, J.A., Zimin, A.V., 2004. Four-dimensional ensemble Kalman Filtering. Tellus 56A, 273–277.

Kalnay, E., 2003. Atmospheric Modeling, Data Assimilation and Predictability. Cambridge University Press, Cambridge 364 pp.

Kalnay, E., Li, H., Miyoshi, T., Yang, S.-C., Ballabrera, J., 2007. 4-D-Var or Ensemble Kalman Filter? Tellus 59A, 758–773, http://dx.doi.org/10.1111/j.1600-0870.2007.00261.x.

Kang, J.-S., Kalnay, E., Liu, J., Fung, I., Miyoshi, T., Ide, K., 2011. Variable localization in an Ensemble Kalman Filter: application to the carbon cycle data assimilation. J. Geophys. Res. 116, http://dx.doi.org/10.1029/2010JD014673.

Keppenne, C.L., Rienecker, M.M., Kurkowski, N.P., Adamec, D.D., 2005. Ensemble Kalman filter assimilation of altimeter and temperature data with bias

Please cite this article as: Gangopadhyay, A., et al., Multiscale forecasting in the western North Atlantic: Sensitivity of model forecast skill to glider data assimilation. Continental Shelf Research (2012), http://dx.doi.org/10.1016/j.csr.2012.09.013

correction and application to seasonal prediction. Nonlinear Processes in Geophysics 12, 491–503.

Kumar, A., Valle-Levinson, A., Atkinson, L.P., 2006. Overrunning of shelf water in the southern Mid-Atlantic Bight. Progress in Oceanography 70, 213–232.

Kunze, E., Dower, J.F., Beveridge, I., Dewey, R., Bartlett, K.P., 2006. Observations of biologically generated turbulence in a coastal inlet. Science 313, 1168–1170, http://dx.doi.org/10.1126/science.1129378.

Lam, F.P., Haley Jr., P.J., Janmaat, J., Lermusiaux, P.F.J., Leslie, W.G., Schouten, M.W., te Raa, L.A., Rixen, M., 2009. At-sea Real-time Coupled Four-dimensional Oceanographic and Acoustic Forecasts during Battlespace Preparation 2007. Special issue of the Journal of Marine Systems on "Coastal processes: Challenges for Monitoring and Prediction", Drs. J.W. Book, Prof. M. Orlic and Michel Rixen (Guest Eds.), 78, S306–S320, http://dx.doi.org/10.1016/j.jmarsys.2009.01.029.

Lermusiaux, P.F.J., 1999. Data assimilation via error subspace statistical estimation, Part II: Mid-Atlantic Bight shelfbreak front simulations and ESSE validation. Monthly Weather Review 127 (8), 1408–1432.

Lermusiaux, P.F.J., 2002. On the mapping of multivariate geophysical fields: sensitivity to size, scales and dynamics. Journal of Atmospheric and Oceanic Technology 19, 1602–1637.

Li, Z., Chao, Y., McWilliams, J.C., Ide, K., 2008a. A three-dimensional variational data assimilation scheme for the regional ocean modeling system. Journal of Atmospheric and Oceanic Technology 25, 2074–2090, http://dx.doi.org/10.1175/2008JTECHO594.1.

Li, Z., Chao, Y., McWilliams, J.C., Ide, K., 2008b. A three-dimensional variational data assimilation scheme for the regional ocean modeling system: implementation and basic experiments. Journal of Geophysical Research-Oceans 113, C05002, http://dx.doi.org/10.1029/2006JC004042.

Lomax, A.S., Corso, W., Etro, J.F. 2005. Employing unmanned aerial vehicles (UAVs) as an element of the Integrated Ocean Observing System. Ocean 2005, Proceedings of the MTS/IEEE. http://dx.doi.org///10.1109/OCEANS.2005.1639759.

Lorenc, A.C., 2003. The potential of the ensemble Kalman Filter for NWP—a comparison with 4D-Var. Quarterly Journal of the Royal Meteorological Society 129, 3183–3203.

Lozano, C.J., Robinson, A.R., Arango, H.G., Gangopadhyay, A., Sloan, N.Q., Haley, P.J., Anderson, L., Leslie, W.G., 1996. An interdisciplinary ocean prediction system: assimilation strategies and structured data models. In: Malanotte-Rizzoli, P. (Ed.), Modern Approaches to Data Assimilation on Ocean Modeling, 61. Elsevier Oceanography Series, Amsterdam, pp. 413–452.

Malanotte-Rizzoli, P. (Ed.), Modern Approaches to Data Assimilation in Ocean Modeling, 61. Elsevier Oceanography Series, Amsterdam, 455 pp.

Miles, T., Glenn, S.M., Schofield, O., Chao, Y., Spatial Variability in Fall Storm Induced Sediment Resuspension on the Mid-Atlantic Bight, Continental Shelf Research, http://dx.doi.org/10.1016/j.csr.2012.08.006, in this issue.

Mooers, C.N.K. (Ed.), 1999. Coastal and Estuarine Studies. AGU, Washington D.C..

Niiler, P.P., Maximenko, N.A., McWilliams, J.C., 2003. Dynamically balanced absolute sea level of the global ocean derived from near-surface velocity observations. Geophysical Research Letters 30 (22), http://dx.doi.org/10.1029/2003GL018628.

Orlanski, I., 1976. A simple boundary condition for unbounded hyperbolic flows. J. Comput. Phys. 21 (3), 251–269.

Ott, E., Hunt, B.R., Szunyogh, I., Zimin, A.V., Kostelich, E.J., Kostelich, M., Corazza, M., Sauer, T., Kalnay, E., Patil, D.J., Yorke, J.A., 2004. A local ensemble Kalman Filter for atmospheric data assimilation. Tellus 56A, 415–428.

Rienecker, M., Keppenne, C., Jacob, J., 2010. GMAO Global Ocean Data Assimilation System. 〈http://www.clivar.org/data/synthesis/projects/GMAO.pdf〉.

Robinson, A.R., Glenn, S.M., Spall, M.A., Walstad, L.J., Gardner, G.M., Leslie, W.G., 1989. Forecasting meanders and rings. EOS Oceanography Report 70 (45), 1464–1473.

Robinson, A.R., Rothschild, B.J., Leslie, W.J., Bisagni, J.J., Borges, M.F., Brown, W.S., Cai, D., Fortier, P., Gangopadhyay, A., Haley Jr., P.J., Kim, H.S., Lanerolle, L., Lermusiaux, P.F.J., Lozano, C.J., Miller, M.G., Strout, G., Sundermeyer, M.A., 2001. The Development and Demonstration of an Advanced Fisheries Management Information System (AFMIS). American Meteorological Society 186–190.

Ryan, J.P., Yoder, J.A., Barth, J.A., Cornillon, P.C., 1999a. Chlorophyll enhancement and mixing associated with meanders of the shelf break front in the Mid-Atlantic Bight. Journal of Geophysical Research 104, 23,479–23,493.

Ryan, J.P., Yoder, J.A., Cornillon, P.C., 1999b. Enhanced chlorophyll at the shelfbreak of the Mid-Atlantic Bight and Georges Bank during the spring transition. Limnology and Oceanography 44, 1–11.

Ryan, J.P., Yoder, J.A., Townsend, D., 2001. Influence of a Gulf Stream warm-core ring on water mass and chlorophyll distributions along the southern flank of Georges Bank. Deep-Sea Research, Part II 48, 159–178.

Schmidt, A.C.K., Brickley, P., Gangopadhyay, A., Cadwallader, M., Sharma, N., Nobre, C., Coholan, P., Feeney, J., 2011. A Feature oriented regional modeling system for the North Brazil current rings migration after retroflection, Proceedings of the Offshore Technology Conference, May 2011, Houston, TX, USA.

Schmidt, A.C.K., Gangopadhyay, A., 2012. An Operational Circulation Ocean Prediction System for the Northwest Atlantic: Validation During July-September of 2006. Continental Shelf Research, http://dx.doi.org/10.1016/j.csr.2012.08.017.

Schofield, O., Bergmann, T., Bissett, W.P., Grassle, F., Haidvogel, D., Kohut, J., Moline, M., Glenn, S., 2002. Linking regional coastal observatories to provide the foundation for a national ocean observation network. Journal of Oceanic Engineering 27 (2), 146–154.

Schofield, O., Glenn, S.M., Irwin, A., Oliver, M., Moline, M.A., Arrott, M., 2012. Earth system monitoring: ocean observatories and information. In: Meyers, R.A., Orcutt, J. (Eds.), Encyclopedia of Sustainability Science and Technology. Springer Science, New York.

Schofield, O., Glenn, S.M., Orcutt, J., Arrott, M., Meisinger, M., Gangopadhyay, A., Brown, W., Signell, R., Moline, M., Chao, Y., Chien, S., Thompson, D., Balasuriya, A., Lermusiaux, P., Oliver, M., 2010. Automated sensor networks to advance ocean science. EOS 91 (39) 28 Sept, 2010.

Schofield, O., Moline, M., Cahill, B., Frazer, T., Kahl, A., Oliver, M., Reinfelder, J., Glenn, S.M., Chant, R. The importance of mixing for phytoplankton productivity in turbid buoyant coastal plumes, Continental Shelf Research, in this issue.

Sherman, J., Davis, R.E., Owens, W.B., Valdes, J., 2001. The autonomous underwater glider "Spray". IEEE Journal of Oceanic Engineering 26, 437–446.

Shulman, I., Kindle, J., Martin, P., deRada, S., Doyle, J., Penta, B., Anderson, S., Chavez, F., Paduan, J., Ramp, S., 2007. Modeling of upwelling/relaxation events with the navy coastal ocean model. Journal of Geophysical Research 112, C06023, http://dx.doi.org/10.1029/2006JC003946.

Shulman, I., Rowley, C., Anderson, S., De Rada, S., Kindle, J., Martin, P., Doyle, J., Cummings, J., Ramp, S., Chavez, F., Fratantoni, D., Davis, R., 2009. Impact of glider data assimilation on the Monterey Bay model. Deep-Sea Research II 56 (2009), 188–198.

Sloan, N.Q.S., 1996. Dynamics of a shelf-slope front, process studies and data-driven simulations in the middle atlantic bight. Ph.D. Thesis, Harvard University, Cambridge, MA.

Stewart, R., Joy, J., 1974. HF Radio Measurements of Surface Currents, in Deep Sea Research and Oceanographic Abstracts, vol. 21. Elsevier, pp. 1039–1049.

Sun, C., Rienecker, M.M., Rosati, A., Harrison, M., Wittenberg, A., Keppenne, C.L., Jacob, J.P., Kovach, R.M., 2007. Comparison and sensitivity of ODASI ocean analyses in the Tropical Pacific. Monthly Weather Review 135, 2242–2264.

Veneziani, M., Edwards, C.A., Doyle, J.D., Foley, D., 2009. A central California coastal ocean modeling study: 1. Forward model and the influence of realistic versus climatological forcing. Journal of Geophysical Research 114, C04015, http://dx.doi.org/10.1029/2008JC004774.

Wang, X., Chao, Y., Thompson, D., Chien, S., Farrara, J., Li, P., Vu Q., Zhang, H., A Coastal Ocean Multi-model Ensemble Forecasting System for Eastern U.S., Continental Shelf Research, http://dx.doi.org/10.1016/j.csr.2012.07.006, in this issue.

Warner, J.C., Sherwood, C.R., Signell, R.P., Harris, C.K., Arango, H.G., 2008. Development of a three-dimensional, regional, coupled wave, current, and sediment-transport model. Computers & Geosciences 34, 1284–1306.

Webb, D.C., Simonetti, P.J., Jones, C.P., 2001. SLOCUM: an underwater glider propelled by environmental energy. IEEE Journal of Oceanic Engineering 26, 447–452.

Weller, R., Toole, J., McCartney, M., Hogg, N., 2000. Outposts in the ocean. Oceanus 42, 20–23.

Wilkin, J.L., Arango, H.G., Haidvogel, D.B., Lichtenwalner, C.S., Durski, S.M., Hedstrom, K.S., 2005. A regional Ocean Modeling System for the Long-term Ecosystem Observatory. Journal of Geophysical Research 110, C06S91, http://dx.doi.org/10.1029/2003JC002218.

Please cite this article as: Gangopadhyay, A., et al., Multiscale forecasting in the western North Atlantic: Sensitivity of model forecast skill to glider data assimilation. Continental Shelf Research (2012), http://dx.doi.org/10.1016/j.csr.2012.09.013